

This article was downloaded by:

On: 25 January 2011

Access details: *Access Details: Free Access*

Publisher *Taylor & Francis*

Informa Ltd Registered in England and Wales Registered Number: 1072954 Registered office: Mortimer House, 37-41 Mortimer Street, London W1T 3JH, UK



Liquid Crystals

Publication details, including instructions for authors and subscription information:

<http://www.informaworld.com/smpp/title~content=t713926090>

The structure and conformation of a mesogenic compound between almost zero and almost complete orientational order

J. W. Emsley^a; G. De Luca^b; A. Lesage^c; D. Merlet^d; G. Pileio^a

^a School of Chemistry, University of Southampton, Southampton SO17 1BJ, UK ^b Dipartimento di Chimica, Università della Calabria, Italy ^c Laboratoire de Chimie, Ecole Normale Supérieure de Lyon, 69364 Lyon, France ^d Equipe de RMN en milieu orienté, ICMMO, UMR 8182, Université de Paris-Sud, 91405 Orsay, France

To cite this Article Emsley, J. W. , De Luca, G. , Lesage, A. , Merlet, D. and Pileio, G.(2007) 'The structure and conformation of a mesogenic compound between almost zero and almost complete orientational order', *Liquid Crystals*, 34: 9, 1071 – 1093

To link to this Article: DOI: 10.1080/02678290701565834

URL: <http://dx.doi.org/10.1080/02678290701565834>

PLEASE SCROLL DOWN FOR ARTICLE

Full terms and conditions of use: <http://www.informaworld.com/terms-and-conditions-of-access.pdf>

This article may be used for research, teaching and private study purposes. Any substantial or systematic reproduction, re-distribution, re-selling, loan or sub-licensing, systematic supply or distribution in any form to anyone is expressly forbidden.

The publisher does not give any warranty express or implied or make any representation that the contents will be complete or accurate or up to date. The accuracy of any instructions, formulae and drug doses should be independently verified with primary sources. The publisher shall not be liable for any loss, actions, claims, proceedings, demand or costs or damages whatsoever or howsoever caused arising directly or indirectly in connection with or arising out of the use of this material.

The structure and conformation of a mesogenic compound between almost zero and almost complete orientational order

J.W. EMSLEY*†, G. DE LUCA‡, A. LESAGE§, D. MERLET¶ and G. PILEIO†

†School of Chemistry, University of Southampton, Southampton SO17 1BJ, UK

‡Dipartimento di Chimica, Università della Calabria, 87030 Arcavacata di Rende, Italy

§Laboratoire de Chimie, Ecole Normale Supérieure de Lyon, 69364 Lyon, France

¶Equipe de RMN en milieu orienté, ICMMO, UMR 8182, Université de Paris-Sud, 91405 Orsay, France

(Received 30 March 2007; accepted 28 June 2007)

The conformational distributions in molecules that form liquid crystalline phases are predicted to depend strongly on orientational order. Results are presented here to test this hypothesis. The mesogen 4-hexyloxy-4'-cyanobiphenyl (6OCB) has been studied by NMR spectroscopy in the isotropic phase and in the nematic phase. In the isotropic phase the field-induced orientational ordering produces small dipolar couplings between ^{13}C and ^1H nuclei, which were determined from the ^{13}C spectra. Couplings between ^1H nuclei were also obtained using 2D selective refocusing experiments. In the nematic phase, both ^1H - ^1H dipolar couplings and quadrupolar splittings for deuterium nuclei were measured for partially-deuterated samples. Both proton and deuterium spectra were also obtained for 6OCB in an equimolar mixture with 4-(ethoxybenzylidene)-4'-butylaniline (EBBA). This mixture exhibits SmA and SmB phases. The data obtained from these experiments has been analysed to yield the probability distribution of the conformations in this molecule generated by rotations about bonds. It is found that there is a substantial influence of the orientational order of the molecules on these distributions.

1. Introduction

All the molecules that form liquid crystalline phases have an anisotropic shape, and are flexible. The flexibility is important in lowering the temperatures of the transitions between both the solid to liquid crystal, T_m , and the liquid crystalline to isotropic liquid T_1 . The conformational distribution, $P(\phi_k)$, generated by rotations through angles ϕ_k about bonds, may change at both T_1 and T_m . The change at T_m is usually the most dramatic when the solid phase is crystalline, since in these phases there is usually just a single minimum energy conformation that is populated. There can be many conformations present in both liquid crystalline and isotropic phases, but it is expected [1] that the conformational distribution in the liquid crystal phase, $P_{LC}(\phi_k)$, will differ from that in the isotropic phase, $P_{iso}(\phi_k)$, because of a relatively large anisotropic contribution, $U_{aniso}(\alpha, \beta, \gamma, \phi_k)$, to the total mean intermolecular potential energy $U_{LC}(\alpha, \beta, \gamma, \phi_k)$; the Euler angles (α, β, γ) are those required to transform from an axis frame fixed in the molecule to one fixed to the director. The difference between $P_{LC}(\phi_k)$ and

$P_{iso}(\phi_k)$ will increase as the orientational order, which itself depends on $U_{aniso}(\alpha, \beta, \gamma, \phi_k)$, increases.

This general phenomenon can be quantified, in principle, by NMR spectroscopy [2] by comparing observed values of dipolar couplings, D_{ij} , or quadrupolar splittings, Δv_i , with values calculated from

$$D_{ij} = \int P_{LC}(\phi_k) D_{ij}(\phi_k) d\phi_k \quad (1)$$

or,

$$\Delta v_i = \int P_{LC}(\phi_k) \Delta v_i(\phi_k). \quad (2)$$

The dependence of $D_{ij}(\phi_k)$ and $\Delta v_i(\phi_k)$ on ϕ_k must be predicted from the known, or assumed, structure of the molecule, and the measured or calculated values of the deuterium quadrupolar tensors. The initial applications of this NMR method to alkyl- [2] or alkyloxycyanobiphenyls [3] analysed the deuterium quadrupolar couplings measured on partially-deuterated compounds, and gave encouraging results. For each $\text{X}_{k-3}-\text{X}_{k-2}-\text{X}_{k-1}-\text{X}_k$ fragment, where $\text{X}=\text{C}$ or O , it was assumed that rotation about the $\text{X}_{k-2}-\text{X}_{k-1}$ bond is such that only the *trans* (*t*) and *gauche+* (*g+*) and *gauche-* (*g-*) minimum

*Corresponding author. Email, J.W.Emsley@soton.ac.uk

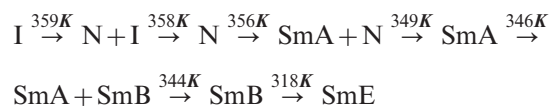
energy forms are populated. It was also found that a very simple model was sufficient to fit the data, which assumed the energy difference, E_{Ig} , between *trans* and *gauche* conformations is independent of the position in the chain. The method of analysis yielded $P_{LC}(n)$, the discrete distribution, and also $P_{iso}(n)$, a distribution that would occur at the same temperature, but without any molecular orientational order. It was found that $P_{LC}(n)$ differs very appreciably from $P_{iso}(n)$ at all temperatures in the mesophase, the differences increasing as temperature is decreased.

Subsequent experiments [4] identified a problem for the nematogen 4-hexyloxy-4'-cyanobiphenyl (6OCB) in that the values of dipolar couplings between ^{13}C and ^1H nuclei, obtained by the separated local field experiment, suggest that the assignment of quadrupolar splittings to chain positions used by Counsell *et al.* [3] is incorrect. The latter assumed that $\Delta\nu_k$ decreases monotonically along the chain, whereas the values of $^1D_{CH}$ measured by Poon *et al.* [4] suggested that there is a reversal of this trend at positions 3 and 4. The values of $\Delta\nu_3$ and $\Delta\nu_4$ were definitively assigned later by synthesizing a compound with deuterons at positions 4–6 in 6OCB [5]. Small changes to the model being used to fit the data could not reproduce this reversal in the order of the splittings.

We report here some new experiments and quantum chemical calculations on 6OCB, one aim of which is to

understand the failure of the model used to interpret the previous data to obtain the correct site dependence of the quadrupolar couplings. A second aim is to test the prediction that the conformational distribution $P_{LC}(\phi_k)$ is strongly dependent on orientational order. To do this NMR data is collected on 6OCB in the nematic phase, and also in the isotropic phase when it was possible to measure field-induced values of $^1D_{CH}$ at each site in the molecules, and $^2D_{HH}$ at positions 25 and 26 in the chain (see figure 1 for atomic labelling). The field-induced order parameters for the molecules in the isotropic phase are $\sim 10^{-3}$ of those in the nematic phase, which allows us to measure a conformational distribution $P_{LC}(\phi_k)$ that is essentially identical to $P_{iso}(\phi_k)$.

We also have measured ^1H and ^2H NMR spectra of 6OCB- d_{15} in an equimolar mixture with EBBA (see figure 1). This mixture has a phase sequence on cooling of:



The orientational order in the SmB phase is approaching the maximum possible in a liquid crystalline phase (S_{zz} , the largest component of the order tensor, $\rightarrow 1.0$), and analysing the set of quadrupolar and dipolar splittings that are obtained yields a conformational distribution for maximum order.

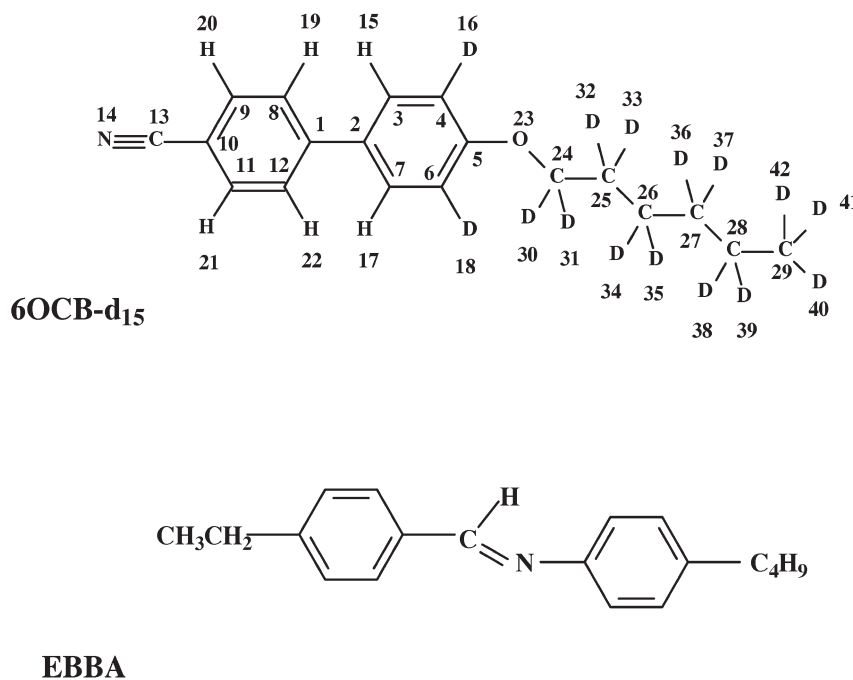


Figure 1. Structures of the deuterated sample of 6OCB- d_{15} and EBBA.

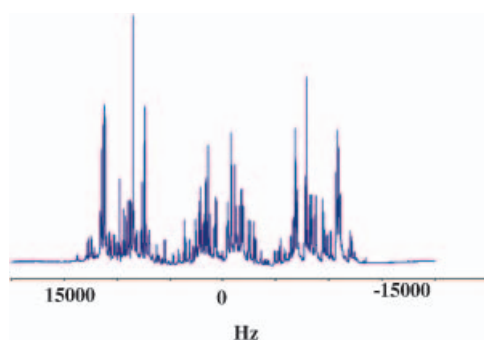


Figure 2. 300 MHz $^1\text{H}\{-^2\text{H}\}$ spectrum of 6OCB- d_{15} recorded at 323 K. The spectrum is a result of Fourier transforming an average of 400 free induction decays, which were stored in 4 k of computer memory. The spectral width is 40 kHz.

2. Experimental

2.1. Spectra of pure 6OCB samples in the nematic phase

A sample of partially-deuterated 6OCB was available from previous studies. The $^1\text{H}\{-^2\text{H}\}$ and ^2H spectra of 6OCB- d_{15} were recorded at a temperature of 323 K, which is 25 K below the nematic to isotropic phase transition, on a Varian spectrometer operating at 300 MHz (figures 2–3). The spectra were recorded with a solenoid probe tuned simultaneously to proton and deuterium frequencies.

Analysis of the proton spectrum using the iterative computer program ARCANA [6] yielded the data shown in table 1. The quadrupolar splittings were obtained from the deuterium spectrum by fitting the peaks with the appropriate number of lines for CD_2 and

Table 1. Dipolar couplings, D_{ij} , and chemical shifts, ν_k , for the protons in 6OCB- d_{15} obtained by analysis of the 300 MHz spectrum recorded in the nematic phase at 323 K.

| i, j | D_{ij}/Hz | J_{ij}^a/Hz |
|--------|--------------------|----------------------|
| 15, 17 | 460.2 ± 1.4 | 2.0 |
| 15, 19 | -2174.3 ± 0.9 | |
| 15, 20 | -451.6 ± 1.1 | |
| 19, 20 | -5259.8 ± 1.0 | 8.0 |
| 19, 21 | 67.9 ± 1.0 | |
| 19, 22 | 466.0 ± 2.3 | 2.0 |
| 20, 21 | 455.9 ± 2.8 | 2.0 |
| 20, 22 | 67.9 ± 1.0 | |

Chemical shifts, ν_k/Hz

| k | ν_k |
|-----|-----------------|
| 15 | 0.0 ± 2.7 |
| 19 | 5.3 ± 2.5 |
| 20 | 135.9 ± 2.0 |

^aThe values of J_{ij} are taken from Brugel [7].

CD_3 groups, each with a Gaussian line shape. However, the dipolar couplings were obtained only with low precision and are not used in the conformational analysis. The values obtained for the quadrupolar splittings are shown in table 2.

2.2. Spectra from a 1:1 mixture of 6OCB- d_{15} and EBBA

$^1\text{H}\{-^2\text{H}\}$ and ^2H spectra were obtained on the 300 MHz Varian spectrometer from a 1:1 molar mixture of 6OCB- d_{15} with 4-ethoxybenzylidene-4'-butylaniline (EBBA) at temperatures of 347 K, when the sample is in the SmA phase (figures 4–5), and at 337 K and 327 K, when it is in a SmB phase (see figures 6–7).

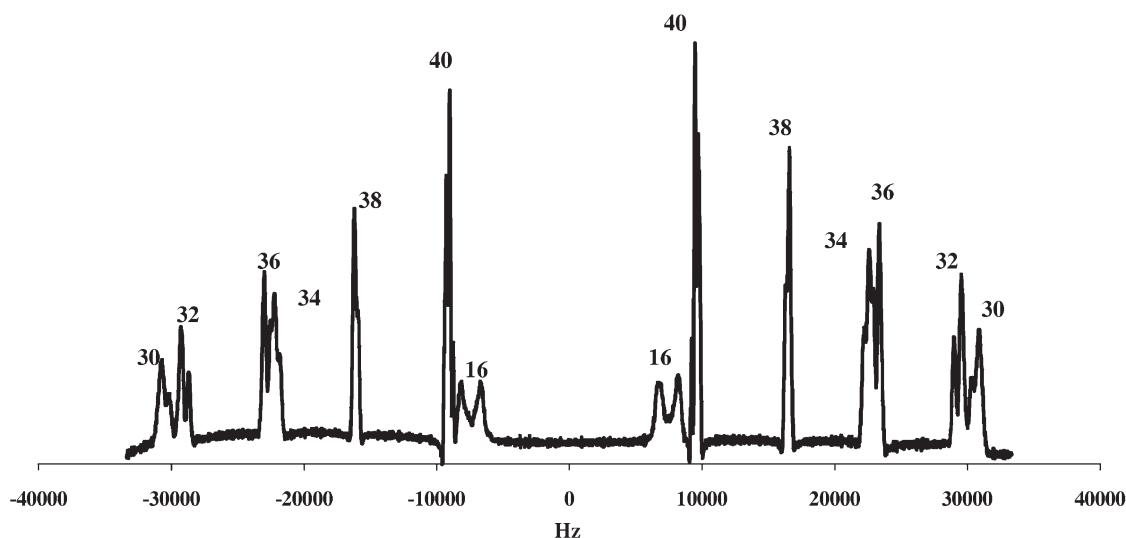


Figure 3. 46.0 MHz ^2H spectrum of 6OCB- d_{15} recorded in the nematic phase at 323 K. The spectrum has a spectral width of 66.7 kHz and is the result of Fourier transforming 400 free induction decays, which were accumulated into 4096 computer locations.

Table 2. Quadrupolar splittings, $\Delta\nu_k$, obtained from the 46.0 MHz deuterium spectrum of 6OCB- d_{15} in the nematic phase at 323 K.

| k | $\Delta\nu_k/\text{Hz}$ |
|-----|-------------------------|
| 16 | $-14\,861 \pm 40$ |
| 30 | $-61\,334 \pm 25$ |
| 32 | $-58\,256 \pm 25$ |
| 34 | $-44\,626 \pm 25$ |
| 36 | $-46\,115 \pm 25$ |
| 38 | $-32\,646 \pm 25$ |
| 40 | $-18\,741 \pm 25$ |

The analysis of the proton and deuterium spectra gave the data in tables 3 and 4.

The SmB phase extends for approximately 26 K and deuterium spectra of the mixture were recorded over the whole of this range. There is only a small, barely detectable change in the deuterium spectrum when the sample first enters the SmE phase. To detect more easily this phase transition the sample in the SmB phase is rotated through an angle θ about an axis perpendicular to the magnetic field. The directors also rotate through the same angle, and they remain at this orientation. All the anisotropic interactions are scaled by the factor $R = \frac{1}{2}(3\cos^2\theta - 1)$. There is a broadening of the lines, which is a consequence of there being a small spread in the directors at the initial orientation, but this broadening is a minimum when $\theta = 0^\circ$ and 90° . On entering the SmE phase, the spectrum becomes a broad, unresolved, distribution of lines, making this transition easy to detect. The broadening of the spectrum in the SmE phase is because the major director is uniformly aligned at 90° to B_0 , but the two minor axes of this biaxial phase are randomly distributed in the plane orthogonal to the field direction. The deuterium spectra for the sample in the SmB phase are shown in figure 6. The quadrupolar splittings and dipolar couplings obtained from the deuterium spectra at 337 K and 327 K are given in table 5.

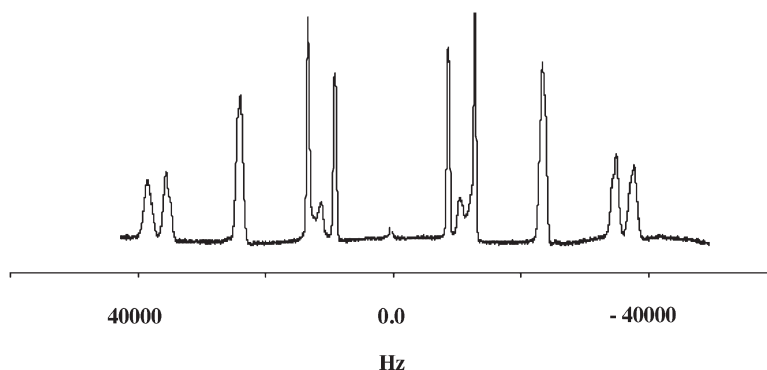


Figure 5. 46.0 MHz ^2H spectrum of 6OCB- d_{15} in a 1:1 mixture with EBBA at 347 K when the sample is in a SmA phase. The spectrum has a spectral width of 100 kHz and is the result of Fourier transforming 400 free induction decays, which were accumulated into 4096 computer locations.

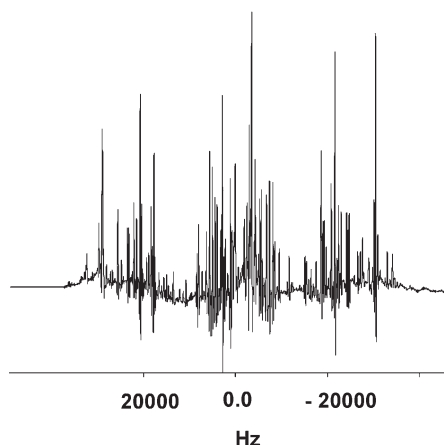


Figure 4. 300 MHz $^1\text{H}\{-^2\text{H}\}$ spectrum of 6OCB- d_{15} in a 1:1 mixture with EBBA at 347 K when the sample is in a SmA phase. The spectrum is the result of averaging 400 free induction decays stored in 4 k of memory and with a spectral width of 100 kHz.

The ratio $\Delta\nu(\theta=90^\circ)/\Delta\nu(\theta=0^\circ)$ should be $-\frac{1}{2}$, and for the data recorded at both temperatures this is correct to a precision of better than 0.2%.

$^1\text{H}\{-^2\text{H}\}$ spectra were recorded and analysed for $\theta=0^\circ$ and 90° when the temperature was 337 K and just for $\theta=90^\circ$ for 327 K. In this case, the main advantage in recording proton spectra with $\theta=90^\circ$ is that less power, and hence less heating, is used for good deuterium decoupling. The spectra are shown in figure 7, and the data obtained from their analysis are given in table 6.

2.3. Spectra measured on a sample of pure 6OCB in the isotropic phase

In contrast to the spectra recorded on samples in the liquid crystalline phases, where the maximum molecular orientational order parameters are >0.5 , it is also possible to obtain NMR data on a sample with very

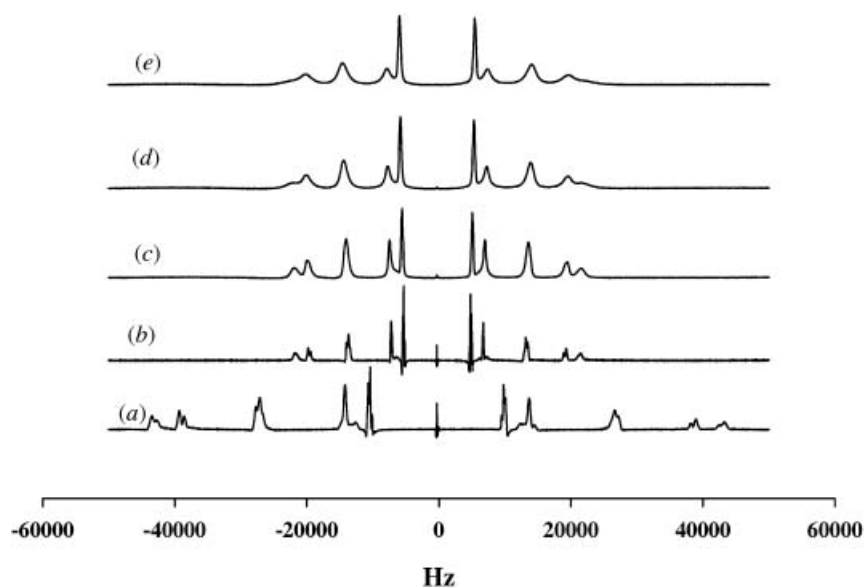


Figure 6. 46.0 MHz ^2H spectra of a 1:1 mixture of 6OCB- d_{15} and EBBA. All the spectra are for the SmB phase. Spectrum (A) is for 343 K and the directors uniformly aligned along the magnetic field direction. Spectra (B)–(E) have the directors aligned perpendicular to B_0 and are at temperatures (B) 343 K, (C) 333 K (D) 323 K and (E) 318 K. All the spectra were accumulated into 4 k of store and have a spectral width of 100 kHz.

small, $<10^{-3}$, order parameters. This was achieved by recording spectra in the isotropic phase of 6OCB in the presence of a magnetic field strength of 16.44 T, corresponding to proton resonance at 700 MHz on a Bruker spectrometer. When $T \gg T_{\text{NI}}$, the magnetic field acts on individual molecules, and the resulting induced dipolar couplings, $D_{ij}^{\text{induced}}(T)$, depend on $\Delta\chi_{\text{mol}}$, the anisotropy in the molecular magnetic susceptibility, and B_0^2 . In the present case the values of $D_{ij}^{\text{induced}}(T)$ are too small to be resolved when

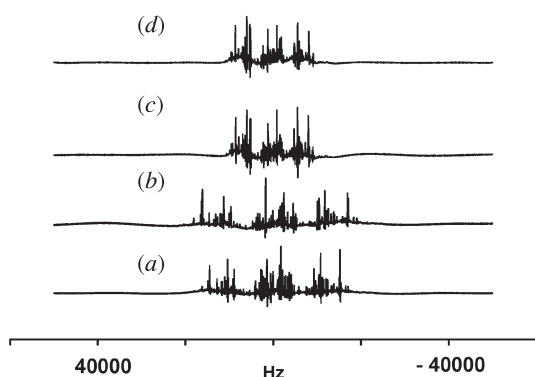


Figure 7. 300 MHz $^1\text{H}\{-^2\text{H}\}$ spectra of a 1:1 mixture of 6OCB- d_{15} and EBBA at (A) 347 K in the SmA phase, (B) 337 K in the SmB phase, (C) and (D) are the same as (B) and (A), but with sample rotated by 90° about an axis perpendicular to the field direction. The spectra were in each case the result of Fourier transforming 400 free induction decays which were accumulated into 4 k of store, with a spectral width of 100 kHz.

Table 3. Dipolar couplings, D_{ij} , and chemical shifts, ν_k , for the protons in 6OCB- d_{15} in a 1:1 mixture with EBBA obtained by analysis of the 300 MHz $^1\text{H}\{-^2\text{H}\}$ spectrum recorded in the SmA phase at 347 K.

| i, j | D_{ij}/Hz | $J_{ij}^{\text{a}}/\text{Hz}$ |
|--------|--------------------|-------------------------------|
| 15, 17 | 614.4 ± 1.7 | 2.0 |
| 15, 19 | -3139.9 ± 1.0 | |
| 15, 20 | -584.4 ± 1.0 | |
| 19, 20 | -6799.6 ± 1.2 | 8.0 |
| 19, 21 | 101.9 ± 1.4 | |
| 19, 22 | 631.1 ± 1.5 | 2.0 |
| 20, 21 | 619.2 ± 1.5 | 2.0 |

Chemical shifts, ν_k/Hz

| k | ν_k |
|-----|-----------------|
| 15 | 0.0 ± 0.9 |
| 19 | 3.4 ± 1.5 |
| 20 | 210.4 ± 1.3 |

^aThe values of J_{ij} are taken from Brugel [7].

Table 4. Quadrupolar splittings, $\Delta\nu_k$, obtained from the 46.0 MHz deuterium spectrum of the deuteriums in 6OCB- d_{15} in the 1:1 mixture with EBBA and in the SmA phase at 347 K.

| k | $\Delta\nu_k/\text{Hz}$ |
|-----|-------------------------|
| 16 | $-23\,546 \pm 40$ |
| 30 | $-75\,209 \pm 25$ |
| 32 | $-70\,294 \pm 25$ |
| 34 | $-47\,380 \pm 50$ |
| 36 | $-48\,164 \pm 50$ |
| 38 | $-26\,207 \pm 25$ |
| 40 | $-17\,735 \pm 25$ |

Table 5. Quadrupolar splittings, $\Delta\nu_k$, obtained from the 46.0 MHz spectrum of the deuteriums in 6OCB- d_{15} in the 1:1 mixture with EBBA and in the SmB phase at 337 and 327 K. Data are given for the sample director aligned along the magnetic field ($\theta=0^\circ$) and at 90° .

| k | $T=337\text{ K}$ | | $T=327\text{ K}$ | |
|-----|-------------------------|-------------------|-------------------------|-------------------|
| | $\Delta\nu_k/\text{Hz}$ | | $\Delta\nu_k/\text{Hz}$ | |
| | $\theta=0^\circ$ | $\theta=90^\circ$ | $\theta=0^\circ$ | $\theta=90^\circ$ |
| 16 | $-26\,911 \pm 40$ | $13\,430 \pm 15$ | $-27\,185 \pm 40$ | $13\,623 \pm 40$ |
| 30 | $-84\,951 \pm 25$ | $42\,447 \pm 25$ | $-86\,568 \pm 25$ | $43\,085 \pm 25$ |
| 32 | $-76\,711 \pm 25$ | $38\,360 \pm 25$ | $-77\,977 \pm 25$ | $38\,925 \pm 25$ |
| 34 | $-51\,969 \pm 50$ | $25\,995 \pm 25$ | $-53\,818 \pm 50$ | $26\,755 \pm 25$ |
| 36 | $-53\,236 \pm 50$ | $26\,617 \pm 25$ | $-54\,832 \pm 50$ | $27\,468 \pm 25$ |
| 38 | $-26\,817 \pm 25$ | $13\,415 \pm 25$ | $-27\,881 \pm 25$ | $13\,928 \pm 25$ |
| 40 | $-19\,526 \pm 25$ | $9\,766 \pm 25$ | $-20\,485 \pm 25$ | $10\,244 \pm 25$ |

$T-T_{\text{NI}}=48\text{ K}$. However, when T_{NI} is approached there is a development of orientational ordering of the molecules, which enhances the values of the induced couplings, which follow the relationship

$$D_{ij}^{\text{induced}}(T) = a_{ij}/(T - T^*), \quad (3)$$

where a_{ij} is a constant for a particular coupling constant, and T^* is of the order of 1 K less than T_{NI} [8]. ^{13}C spectra were recorded from $T-T_{\text{NI}}=48\text{ K}$ down to 0.1 K, and $^1\Delta_{\text{CH}}(T)$, the splittings between the peaks in each chemically-shifted multiplet were measured. These are related to $^1D_{\text{CH}}^{\text{induced}}(T)$ and $^1J_{\text{CH}}$ by

$$^1\Delta_{\text{CH}} = 2^1D_{\text{CH}}^{\text{induced}}(T) + ^1J_{\text{CH}}. \quad (4)$$

The values of $^1J_{\text{CH}}$ were obtained from the spectra at $T-T_{\text{NI}}=48\text{ K}$. The assignment of the peaks in both ^{13}C

and ^1H spectra was achieved using a 2D HMBC spectrum [8]. It was also possible to obtain induced dipolar couplings, $^nD_{\text{HH}}^{\text{induced}}$, between some of the protons from the ^1H spectra. Figure 8 shows proton spectra taken at values of $T-T_{\text{NI}}$ of 48.1 K and 0.1 K.

Note the marked change in shape of the peak from the protons H30, H31. At the higher temperature the peak has a triplet structure from spin-spin scalar coupling to the protons H32, H33. At the lower temperature the presence of a dipolar coupling $^2D_{30,31}^{\text{induced}}$ has a significant effect on the peak shape, but it is not possible to extract this coupling directly. The coupling can be obtained by performing a 2D selective refocusing experiment (SERF) [8, 9], which gives the result shown in figure 9, and the projection of which on to the F1 axis is a doublet with separation $3^2D_{30,31}^{\text{induced}}$. A

Table 6. Dipolar couplings, D_{ij} , and chemical shifts, δ_k , for the protons in 6OCB- d_{15} in a 1:1 mixture with EBBA obtained by analysis of the 300 MHz $^1\text{H}-\{^2\text{H}\}$ spectra recorded in the SmB phase at 337 and 327 K. Data are given for both the directors aligned parallel to the magnetic field, $\theta=0^\circ$, and perpendicular, $\theta=90^\circ$, for 337 K, and just for $\theta=90^\circ$ for 327 K.

| i, j | $T=337\text{ K}$ | | $T=327\text{ K}$ | |
|--------|--------------------|-------------------|----------------------|-----|
| | D_{ij}/Hz | | J_{ij}^a/Hz | |
| | $\theta=0^\circ$ | $\theta=90^\circ$ | $\theta=90^\circ$ | |
| 15, 17 | 682.5 ± 1.5 | 346.0 ± 1.8 | -345.0 ± 1.2 | 2.0 |
| 15, 19 | -3663.9 ± 0.7 | 1834.4 ± 0.9 | 1857.8 ± 0.7 | |
| 15, 20 | -643.6 ± 0.8 | 319.7 ± 1.1 | 321.3 ± 1.2 | |
| 19, 20 | -7386.6 ± 1.0 | 3695.2 ± 1.1 | 3714.0 ± 1.1 | 8.0 |
| 19, 21 | 120.0 ± 1.1 | -56.2 ± 1.2 | -60.2 ± 1.2 | |
| 19, 22 | 696.1 ± 1.0 | -346.0 ± 2.5 | -345.0 ± 1.2 | 2.0 |
| 20, 21 | 682.1 ± 1.0 | -335.0 ± 2.9 | -349.4 ± 1.2 | 2.0 |

| Chemical shifts/Hz | |
|--------------------|--------------------------------|
| k | $(\nu_k - \nu_{15})/\text{Hz}$ |
| 15 | 0.0 |
| 19 | 10 ± 2.3 |
| 20 | 248 ± 2.1 |

^aThe values of J_{ij} are taken from Brugel [7].

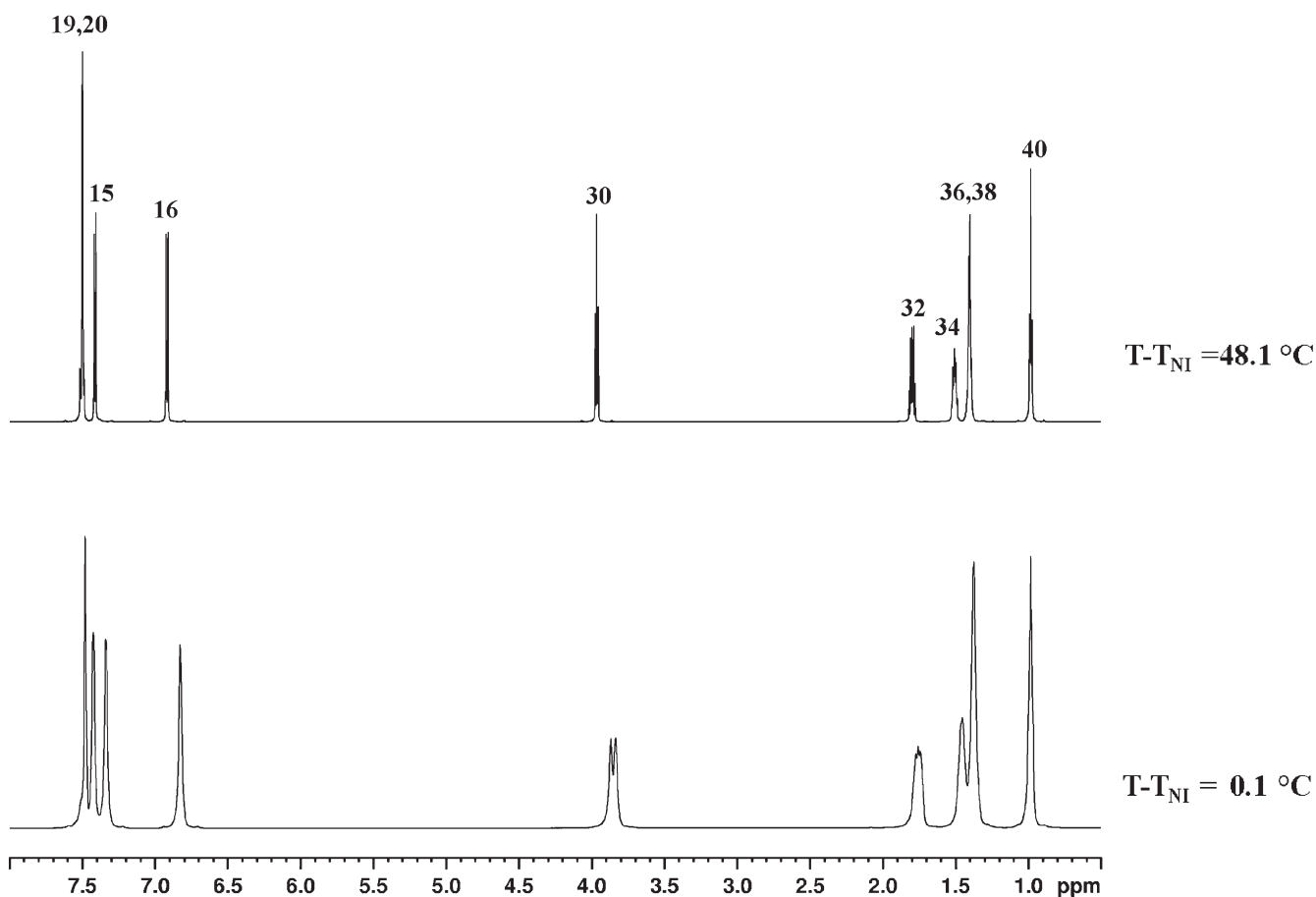


Figure 8. 700 MHz ^1H spectrum of 6OCB in the isotropic phase at values of $T - T_{\text{NI}}$ of 48.1 K and 0.1 K.

similar SERF experiment was also possible on the peak from H32, H33 to give $3^2D_{32,33}^{\text{induced}}$. All the induced couplings obtained for 6OCB at $T - T_{\text{NI}} = 0.1$ K are given in table 7.

3. Quantum chemical calculations

3.1. The structure

In order to relate the NMR data to the conformational distributions of the molecules in the liquid crystalline phases it is useful to have a good estimate of the structure of an isolated 6OCB molecule in the minimum energy structure, and of the relative energies of other minimum energy structures which an isolated molecule may adopt by virtue of rotations about the bonds. Calculations of the structure of the minimum energy structure were carried out with the *ab initio* molecular orbital method MP2, using the basis set 6-31G*, and also with the density functional method B3LYP, with both 6-31G* and 6-311G** basis sets. The calculations were done using the Gaussian 03 software [10]. The results are shown in table 8. The bond lengths and

angles predicted by the three calculations are in close agreement, except for the values of the dihedral angle τ_{8123} , the ring torsion angle. The MP2/6-31G* calculation predicts a value of $\tau_{8123} = 43.168^\circ$, whereas the B3LYP functional with the same basis set gives $\tau_{8123} = 35.345^\circ$, and using the extended basis of 6-311G** increases this to $\tau_{8123} = 37.172^\circ$. Calculations with the B3LYP functional seem to consistently over-emphasize the importance of π -conjugation in molecules. For example, calculations [11] on biphenyl by MP2/6-31G* predicted a torsional angle of 44.62° , whereas B3LYP/6-31+G(d) gives 40.35° . Experiment favours 44° for this compound in the gas phase [12]. In some cases the B3LYP DFT approach fails to obtain the correct location of the global minimum for rotation of two conjugated fragments in a molecule. Thus, for styrene, for which the global minimum is with the phenyl ring at a non-zero angle to the olefinic group, DFT calculations predict a planar minimum structure [13]. Calculations [14] by MP2/6-311++G** find the minimum at 27° , and a liquid crystal NMR study [15] found 18° .

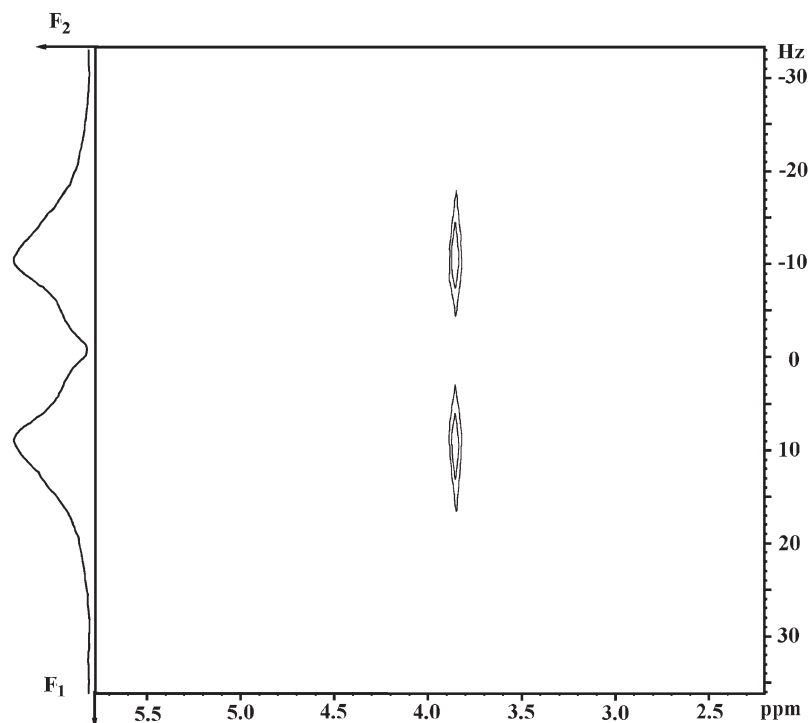


Figure 9. 700 MHz ^1H selective refocusing experiment on protons H30, H31 in 6OCB in the isotropic phase at $T-T_{\text{NI}}=0.1$ K.

However, for large molecules the DFT calculations are possible with modest computational resources, whereas MP2 calculations become prohibitively long. The molecule 6OCB is just at the limit, for our computational resource, at which both calculations are feasible, although with a smaller basis set for MP2.

The dipolar couplings between protons in the biphenyl fragment will be used to determine the ring torsion angle in 6OCB. There is insufficient data to determine the minimum energy positions for rotation

Table 7. Induced dipolar couplings $^1D_{\text{CH}}^{\text{induced}}$ and $^2D_{\text{HH}}^{\text{induced}}$ obtained at $T-T_{\text{NI}}=0.1$ K for 6OCB in the isotropic phase at 16.44 T.

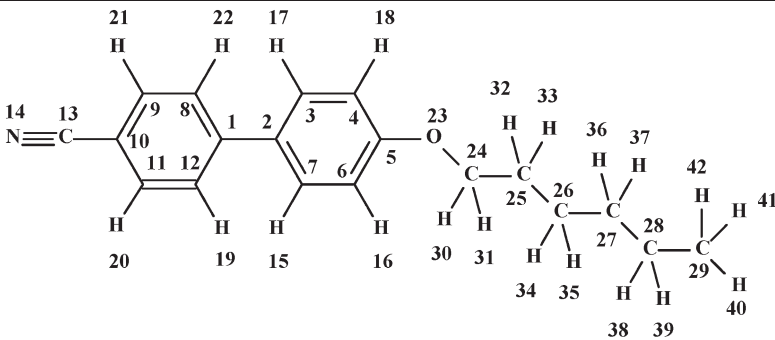
| Nuclei | $^1D_{\text{CH}}^{\text{induced}}/\text{Hz}$ | $^2D_{\text{HH}}^{\text{induced}}/\text{Hz}$ |
|----------------------|--|--|
| 9, 20=11, 21 | 2.90 ± 0.05 | |
| 8, 19=12, 22 | 4.15 ± 0.05 | |
| 3, 15=7, 17 | 2.90 ± 0.05 | |
| 4, 16=6, 18 | 2.25 ± 0.05 | |
| 24, 30=24, 31 | 10.32 ± 0.05 | |
| 25, 32=25, 33 | 9.27 ± 0.05 | |
| 26, 34=26, 35 | 7.60 ± 0.05 | |
| 27, 36=27, 37 | 7.75 ± 0.05 | |
| 28, 38=28, 39 | 4.58 ± 0.05 | |
| 29, 40=29, 41=29, 42 | 2.50 ± 0.05 | |
| 30, 31 | | 6.60 ± 0.05 |
| 32, 33 | | 6.20 ± 0.05 |

about the other bonds in the molecule and so these have been calculated by the B3LYP/6-311G** method, using full geometry optimisation. The positions of the minimum energy structures are given in table 9.

Rotation about C5–O23 is very similar to that in anisole in having minima with the C24–O23 bond in the plane of the attached ring [16, 17]. Rotation about the C24–O23 bond gives rise to local minima at $\pm 85.0^\circ$, which are 6.2 kJ mol^{-1} higher in energy than the *trans* form. To explore this further calculations were performed by B3LYP/6-31G* with the dihedral angle $\tau_{25,24,23,5}$ fixed at 15° intervals in the range 0° to 180° , with optimization of all other parameters. The resulting rotational potential, $V(\phi)$, is shown in figure 10.

Note that most of the calculations did not fully converge, and that away from the minima at 85° and 180° the structure severely distorts. These calculations, although of an approximate nature, serve to show that rotation about this C–O bond is not a simple single bond rotation, but the minimum energy pathway will involve partial rotations about the neighbouring bonds too. However, in the simplified conformational model which is used to interpret the NMR data it is sufficient to note the position of the minima and their energy separation.

The data in table 9 for rotation about the first C–C bond in the chain, C25–C24, also produces an unusual and unexpected result in that the lowest energy occurs

Table 8. Bond lengths, R_{ij} , bond angles, θ_{ijk} , and dihedral angles, τ_{ijks} , calculated by the MP2/6-31G*, B3LYP/6-31G* and B3LYP/6-311G** methods for 6OCB.


| | | MP2/6-31G* | B3LYP/6-31G* | B3LYP/6-311G** |
|---------------------|------|------------|-----------------------|----------------|
| Bond lengths | | | | |
| i, j | type | | $R_{ij}/\text{\AA}$ | |
| 1, 2 | C–C | 1.475 | 1.481 | 1.481 |
| 2, 3 | C–C | 1.401 | 1.402 | 1.399 |
| 3, 4 | C–C | 1.397 | 1.395 | 1.393 |
| 4, 5 | C–C | 1.400 | 1.401 | 1.398 |
| 5, 6 | C–C | 1.403 | 1.404 | 1.402 |
| 2, 7 | C–C | 1.407 | 1.409 | 1.406 |
| 1, 8 | C–C | 1.405 | 1.408 | 1.405 |
| 8, 9 | C–C | 1.392 | 1.389 | 1.387 |
| 9, 10 | C–C | 1.403 | 1.405 | 1.402 |
| 10, 11 | C–C | 1.403 | 1.405 | 1.402 |
| 11, 12 | C–C | 1.392 | 1.389 | 1.387 |
| 10, 13 | C–C | 1.435 | 1.433 | 1.429 |
| 13, 14 | C–N | 1.184 | 1.164 | 1.156 |
| 3, 15 | C–H | 1.088 | 1.086 | 1.084 |
| 4, 16 | C–H | 1.085 | 1.084 | 1.081 |
| 6, 18 | C–H | 1.087 | 1.086 | 1.084 |
| 7, 17 | C–H | 1.088 | 1.085 | 1.083 |
| 8, 19 | C–H | 1.088 | 1.086 | 1.083 |
| 9, 20 | C–H | 1.087 | 1.085 | 1.083 |
| 11, 21 | C–H | 1.087 | 1.085 | 1.083 |
| 12, 22 | C–H | 1.088 | 1.086 | 1.083 |
| 5, 23 | C–O | 1.368 | 1.361 | 1.359 |
| 23, 24 | O–C | 1.432 | 1.429 | 1.431 |
| 24, 25 | C–C | 1.515 | 1.522 | 1.520 |
| 25, 26 | C–C | 1.528 | 1.534 | 1.533 |
| 26, 27 | C–C | 1.527 | 1.534 | 1.533 |
| 27, 28 | C–C | 1.527 | 1.534 | 1.533 |
| 28, 29 | C–C | 1.526 | 1.532 | 1.531 |
| 24, 30 | C–H | 1.099 | 1.100 | 1.098 |
| 25, 32 | C–H | 1.096 | 1.098 | 1.095 |
| 26, 34 | C–H | 1.098 | 1.100 | 1.098 |
| 27, 36 | C–H | 1.098 | 1.100 | 1.097 |
| 28, 38 | C–H | 1.097 | 1.099 | 1.097 |
| 29, 40 | C–H | 1.094 | 1.096 | 1.093 |
| Bond angles | | | | |
| i, j, k | type | | $\theta_{ijk}/^\circ$ | |
| 1, 2, 3 | CCC | 120.853 | 121.311 | 121.305 |
| 2, 3, 4 | CCC | 121.440 | 121.856 | 121.821 |
| 3, 4, 5 | CCC | 119.460 | 119.708 | 119.755 |
| 4, 5, 6 | CCC | 119.709 | 119.259 | 119.755 |
| 7, 2, 3 | CCC | 118.297 | 117.450 | 117.478 |
| 8, 1, 2 | CCC | 120.737 | 121.138 | 121.128 |
| 1, 8, 9 | CCC | 121.061 | 121.364 | 121.335 |

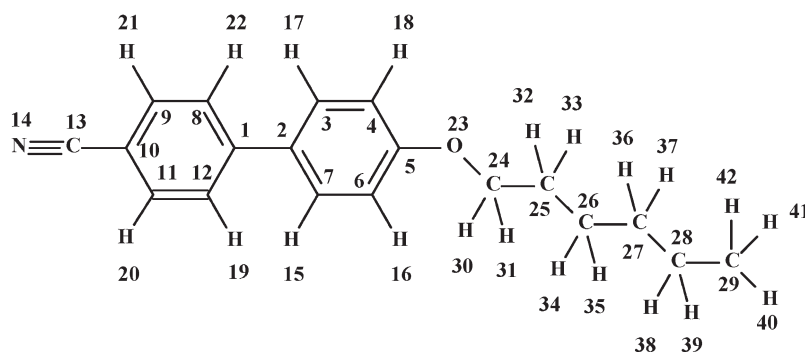
Table 8. (Continued.)

| | | | | |
|------------|-----|---------|---------|---------|
| 8, 9, 10 | CCC | 119.578 | 120.065 | 120.100 |
| 9, 10, 11 | CCC | 120.150 | 119.306 | 119.271 |
| 10, 11, 12 | CCC | 119.581 | 120.048 | 120.084 |
| 9, 10, 13 | CCC | 119.921 | 120.341 | 120.358 |
| 2, 3, 15 | CCH | 119.509 | 119.562 | 119.597 |
| 3, 4, 16 | CCH | 119.200 | 119.308 | 119.257 |
| 2, 7, 17 | CCH | 119.691 | 119.606 | 119.636 |
| 5, 6, 18 | CCH | 118.310 | 118.479 | 118.362 |
| 9, 8, 19 | CCH | 119.579 | 119.141 | 119.133 |
| 8, 9, 20 | CCH | 120.678 | 120.351 | 120.336 |
| 10, 11, 21 | CCH | 119.740 | 119.592 | 119.576 |
| 11, 12, 22 | CCH | 119.557 | 119.135 | 119.129 |
| 4, 5, 23 | CCO | 125.017 | 124.896 | 124.877 |
| 5, 23, 24 | COC | 117.376 | 118.963 | 119.189 |
| 23, 24, 25 | OCC | 107.085 | 107.875 | 107.779 |
| 24, 25, 26 | CCC | 112.100 | 112.397 | 112.474 |
| 25, 26, 27 | CCC | 112.694 | 113.121 | 113.193 |
| 26, 27, 28 | CCC | 113.167 | 113.423 | 113.499 |
| 27, 28, 29 | CCC | 112.719 | 113.164 | 113.229 |
| 23, 24, 30 | OCH | 109.923 | 109.818 | 109.758 |
| 24, 25, 32 | CCH | 108.623 | 108.619 | 108.528 |
| 25, 26, 34 | CCH | 109.575 | 109.534 | 109.535 |
| 26, 27, 36 | CCH | 109.263 | 109.269 | 109.242 |
| 27, 28, 38 | CCH | 109.157 | 109.227 | 109.196 |
| 28, 29, 40 | CCH | 111.432 | 111.397 | 111.413 |
| 28, 29, 41 | CCH | 110.850 | 111.195 | 111.192 |

Dihedral angles

| <i>ijkl</i> | type | $\tau_{ijkl} / ^\circ$ | | |
|----------------|------|------------------------|----------|----------|
| 4, 3, 2, 1 | CCCC | 180.006 | 180.082 | 180.070 |
| 5, 4, 3, 2 | CCCC | -0.115 | 0.140 | 0.183 |
| 6, 5, 4, 3 | CCCC | 0.054 | -0.169 | -0.214 |
| 7, 2, 3, 4 | CCCC | 0.063 | 0.035 | 0.048 |
| 8, 1, 2, 3 | CCCC | 43.168 | 35.345 | 37.172 |
| 9, 8, 1, 2 | CCCC | 180.314 | 180.239 | 180.226 |
| 10, 9, 8, 1 | CCCC | -0.464 | -0.274 | -0.227 |
| 11, 10, 9, 8 | CCCC | 0.167 | 0.091 | 0.055 |
| 12, 11, 10, 9 | CCCC | 0.276 | 0.166 | 0.149 |
| 13, 10, 9, 8 | CCCC | 180.000 | 180.117 | 180.088 |
| 15, 3, 2, 1 | HCCC | 1.891 | 1.913 | 1.804 |
| 16, 4, 3, 2 | HCCC | 180.726 | 180.768 | 180.756 |
| 17, 7, 2, 1 | HCCC | 1.900 | 1.653 | 1.540 |
| 18, 6, 5, 4 | HCCC | 179.234 | 179.335 | 179.342 |
| 19, 8, 9, 10 | HCCC | 178.021 | 178.041 | 178.155 |
| 20, 11, 10, 9 | HCCC | 180.409 | 180.489 | 180.515 |
| 21, 11, 10, 9 | HCCC | 179.367 | 179.445 | 179.455 |
| 22, 12, 11, 10 | HCCC | 178.060 | 178.098 | 178.210 |
| 23, 5, 4, 3 | OCCC | 180.022 | 179.819 | 179.768 |
| 24, 23, 5, 4 | COCC | -0.345 | -1.133 | -1.110 |
| 25, 24, 23, 5 | CCOC | 180.420 | 181.029 | 180.900 |
| 26, 25, 24, 23 | CCCO | 180.032 | 179.356 | 179.186 |
| 27, 26, 25, 24 | CCCC | 179.998 | 179.993 | 179.991 |
| 28, 27, 26, 25 | CCCC | 179.994 | 179.683 | 179.564 |
| 29, 28, 27, 26 | CCCC | 179.992 | 179.993 | 179.980 |
| 30, 24, 23, 25 | HCOC | -120.920 | -120.829 | -120.702 |
| 32, 25, 24, 26 | HCCO | -121.090 | -122.089 | -122.062 |
| 34, 26, 25, 27 | HCCC | -121.789 | -122.059 | -122.036 |
| 36, 27, 26, 28 | HCCC | -122.02 | -122.180 | -122.161 |
| 38, 28, 27, 29 | HCCC | -122.070 | -122.237 | -122.233 |
| 40, 29, 28, 27 | HCCC | 180.012 | 179.934 | 179.967 |
| 41, 29, 28, 27 | HCCC | -59.817 | -59.949 | -59.936 |

Table 9. Positions of the minimum energy forms generated by rotation through an angle ϕ about bonds in 6OCB, and their relative energies, $E_{ig}(i, j)$, calculated with full geometry optimization by B3LYP/6-311G**.



| Bond | Number of minima | Position of minima, $\phi/^\circ$ | $E_{ig}(i, j)$, relative energies of local minimum/ kJ mol^{-1} |
|---------|------------------|-----------------------------------|---|
| C5–O23 | 2 | -0.11 and 179.89 | 0 |
| O23–C24 | 3 | 180.9 | 0 |
| | | 85.0 | 6.2 |
| C24–C25 | 3 | 179.2 | 0 |
| | | 64.1 | -1.0 |
| C25–C26 | 3 | 180.0 | 0 |
| | | 66.6 | 3.6 |
| C26–C27 | 3 | 179.6 | 0 |
| | | 66.2 | 3.4 |
| C27–C28 | 3 | 180.0 | 0 |
| | | 66.6 | 3.5 |

for $\phi = \pm 64.1^\circ$, which are predicted to be 1 kJ mol^{-1} below the $\phi = 180^\circ$ state. This result was checked by investigating the shape of the rotational potential about this bond. The calculations were by the B3LYP/6-31G*

method, and as in the previous case involve doing optimizations of the structure with fixed values of the torsion angle. The resulting bond rotational potential is shown in figure 11. In this case the bond lengths and

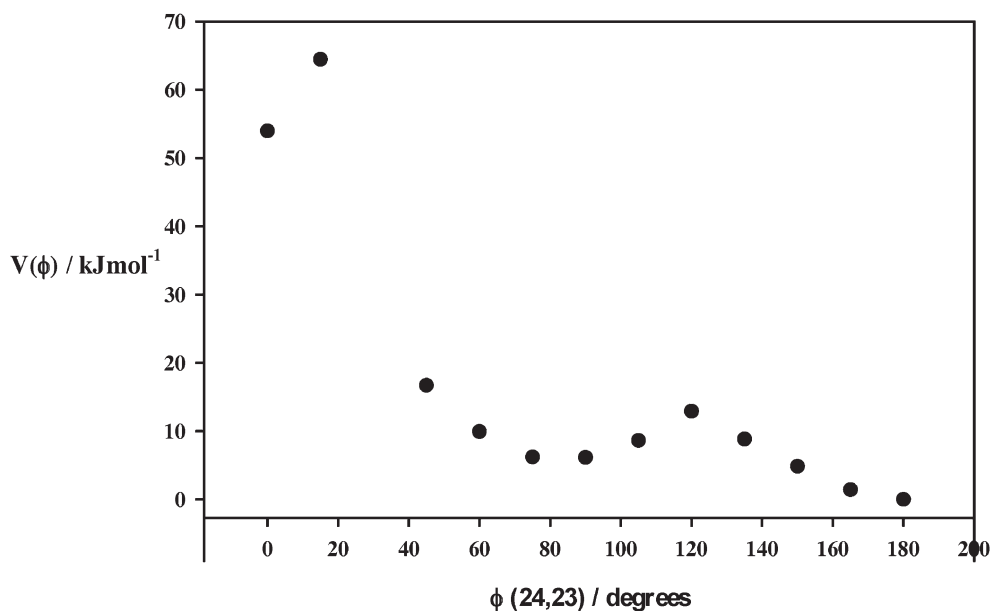


Figure 10. Energy, $V(\phi)$, calculated by B3LYP/6-31G* for rotation about the bond O(23)–C(24) in 6OCB.

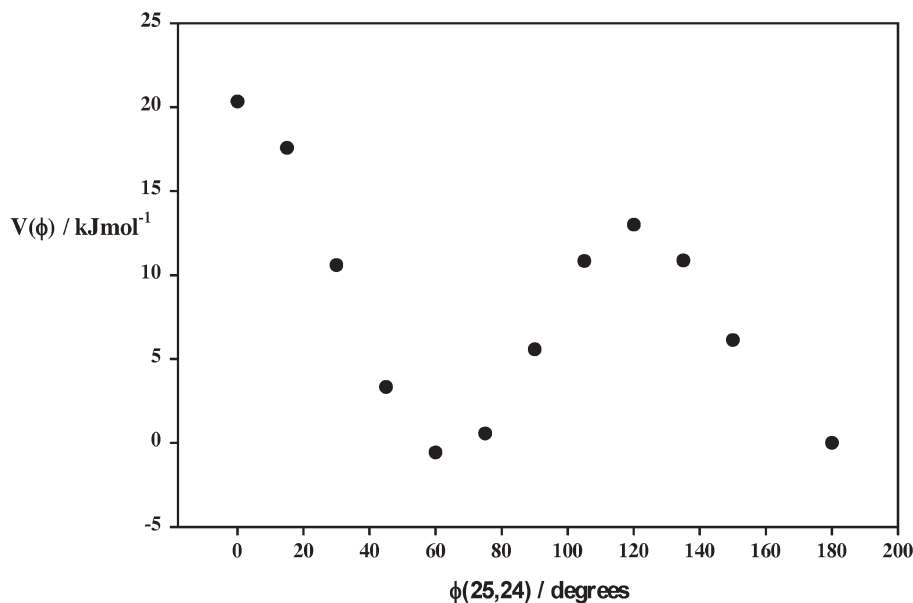


Figure 11. Energy, $V(\phi)$, calculated by B3LYP/6-31G* for rotation about the bond C(24)–C(25) in 6OCB.

angles at the gauche minima are barely changed from that for the trans form.

The positions of the minima and the energy differences ΔE_{tg} for rotation about the bonds C26–C27, C27–C28 and C28–C29 are each very similar to one another and to those expected for C–C bonds in similar alkyl chains.

An X-ray investigation [18] of 6OCB crystals found that the alkyloxy chain is in the fully-extended conformation, and therefore this is the minimum energy conformer in the solid state. This contrasts with the minimum energy conformer for an isolated molecule, as calculated here, being the pair with a gauche link for O–C–C–C.

4. Deuterium quadrupolar tensors

The NMR experiments on the partially deuterated forms of 6OCB yield a splitting, Δv_k , for each non-equivalent labelled site. These are related to values, $\Delta v_k(\phi_k)$, in each of the conformers generated by rotation about the bonds in the alkyloxy chain by equation (2). In the RIS model for the chain conformations this equation is replaced by

$$\Delta v_k = \sum_n^N P_{LC}(n) \Delta v_k(n), \quad (5)$$

where $P_{LC}(n)$ is the probability that the molecules is in the n th conformer out of a total of N . In each conformer the value of $\Delta v_k(n)$ is related to principal components, $q_{\alpha\alpha}(k, n)$ of the deuterium quadrupolar tensor at site k . The principal axes at each site will be labelled a, b , and c , noting that their orientation in a molecule fixed frame

vary with k . Thus,

$$\begin{aligned} \Delta v_k(n) = & \frac{3}{4} q_{aa}(k, n) [S_{zz}(n) \{ (3 \cos^2 \theta_{azk} - 1) + \eta(k, n) (\cos^2 \theta_{bz k} - \cos^2 \theta_{cz k}) \} \\ & + (S_{xx}(n) - S_{yy}(n)) \{ \cos^2 \theta_{axk} - \cos^2 \theta_{ayk} \\ & + \frac{1}{3} \eta(k, n) (\cos^2 \theta_{bxk} - \cos^2 \theta_{byk} - \cos^2 \theta_{cxk} + \cos^2 \theta_{cyk}) \} \\ & + 4S_{xy}(n) \left\{ \cos \theta_{axk} \cos \theta_{ayk} + \frac{1}{3} \eta(k, n) (\cos \theta_{bxk} \cos \theta_{byk} - \cos \theta_{cxk} \cos \theta_{cyk}) \right\} \\ & + 4S_{xz}(n) \left\{ \cos \theta_{axk} \cos \theta_{azk} + \frac{1}{3} \eta(k, n) (\cos \theta_{bxk} \cos \theta_{bz k} - \cos \theta_{cxk} \cos \theta_{cz k}) \right\} \\ & + 4S_{yz}(n) \left\{ \cos \theta_{ayk} \cos \theta_{azk} + \frac{1}{3} \eta(k, n) (\cos \theta_{byk} \cos \theta_{bz k} - \cos \theta_{cyk} \cos \theta_{cz k}) \right\} \end{aligned} \quad (6)$$

Here $q_{aa}(k, n)$ is the principal component of largest magnitude, and the asymmetry parameter is

$$\eta(k, n) = [q_{bb}(k, n) - q_{cc}(k, n)] / q_{aa}(k, n). \quad (7)$$

In order to use equation (6) it is necessary to know the values of the principal components $q_{\alpha\alpha}(k, n)$ and the orientation of the principal axes, given by the angles θ_{azk} etc, in the molecular frame x, y, z , which is fixed in one of the rigid fragments of the molecule, for example one of the phenyl rings in 6OCB.

In previous studies of liquid crystals using experimental quadrupolar splittings the assumptions have been made that $q_{aa}(k, n)$ and $\eta(k, n)$ are independent of n , and that they have identical values for all sites in aromatic fragments, (185 kHz and 0.04 respectively), whilst for all aliphatic sites they are given values of 168 kHz and zero, which are those obtained experimentally for perdeuterated ethane, butane and hexane [19]. The validity of these assumptions is tested here by calculating the magnitude of the principal components, $V_{\alpha\alpha}(k)$, of the electric field gradient tensors for all the

deuterium sites in 6OCB by the B3LYP/6-311G** method. The relationship between $V_{\alpha\alpha}(k)$ and $q_{\alpha\alpha}(k)$ is:

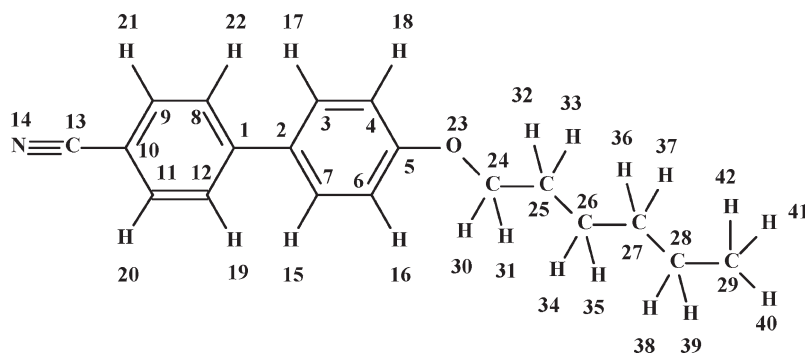
$$q_{\alpha\alpha}(k) = eQ_D V_{\alpha\alpha}(k)/h, \quad (8)$$

where Q_D is the quadrupole moment of the deuterium nucleus. It has been found that using equation (8) for several small molecules, after calculating $V_{\alpha\alpha}(k)$ with either *ab initio* methods such as MP2, or the density functional B3LYP, leads to values of $q_{\alpha\alpha}(k)$ that are consistently too large by about 5%. This was attributed to a combination of such factors as the neglect of vibrational averaging, limitations in the basis sets used, and errors in the experimental values. Bailey [20] quotes a value for the ratio $q_{\alpha\alpha}(k)/V_{\alpha\alpha}(k)$ of 636.5 kHz/a.u., which gives a good fit to the experimental values for a wide range of molecules when using B3LYP/6-31G**. (Note that relating the values of the components of the field gradient tensor as calculated by the program Gaussian 03 in atomic units (a.u) to components of the deuterium quadrupolar tensor in units of frequency requires a negative sign for the conversion factor).

Values of $V_{\alpha\alpha}(k)$ for the various sites in 6OCB have been calculated using the B3LYP/6-311G** method for the molecule in the fully-extended conformer, which were then used to obtain the values of $q_{\alpha\alpha}(k)$ shown in table 10, using the conversion factor -636.5 kHz/a.u. These calculations gave values for $q_{\alpha\alpha}(k)$ that are too large by about 10%, as judged by a comparison with the value of 168 kHz measured for the value of q_{aa} in the deuterated alkanes. The conversion factor was therefore amended to -571.8 kHz/a.u., which brings the calculated values of q_{aa} into closer agreement with the average value of 168 kHz for an aliphatic site. The calculated values of q_{aa} for the aromatic sites are in good agreement with the values determined for biphenyl- d_{10} (181.5 kHz) [21] and 4-cyanobiphenyl- d_9 (178 kHz) [22] dissolved in liquid crystalline solvents.

Calculations were also done using B3LYP/6-31G* and MP2/6-31G*, which gave values in quite good agreement with each other (better than 2%), but about 4% larger than those obtained by B3LYP/6-311G**. All the calculations produce the same general features, thus

Table 10. Values of the principal components, $q_{\alpha\alpha}(k)$ in kHz, of the quadrupole tensor for deuterium at different sites in 6OCB when in the full-extended minimum energy form, calculated using the B3LYP/6-311G** method. The values were obtained using equation (8) with conversion factors of (A) -636.5 kHz/a.u., and (B) -571.8 kHz/a.u.



| Site | q_{aa} | | η |
|-----------------|----------|-------|--------|
| | (A) | (B) | |
| 15 | 201.1 | 180.7 | 0.074 |
| 16 | 206.4 | 185.4 | 0.098 |
| 17 | 201.3 | 180.8 | 0.071 |
| 18 | 202.8 | 182.2 | 0.072 |
| 19 | 201.4 | 180.9 | 0.074 |
| 20 | 200.6 | 180.2 | 0.072 |
| 21 | 200.6 | 180.2 | 0.072 |
| 22 | 201.3 | 180.8 | 0.075 |
| 30 | 181.4 | 163.0 | 0.066 |
| 32 | 187.7 | 168.6 | 0.025 |
| 34 | 186.3 | 167.4 | 0.033 |
| 36 | 186.4 | 167.5 | 0.031 |
| 38 | 187.6 | 168.5 | 0.026 |
| 40 ^a | 192.5 | 173.0 | 0.024 |

^aAverage for the three methyl deuterium sites.

aromatic sites are predicted to have larger values of q_{aa} and η than aliphatic sites, and the relative values within the biphenyl group, and along the chain are very similar. The calculations also agree in placing the principal axis a along the C–D bond to within 0.2° .

The calculations (column (B)) predict that there is an appreciable difference between q_{aa} and η for the two sites 16 and 18, which is because D(16) is closer to the chain protons at positions 30 and 31. The close approach of these atoms also affects the values in the all-trans form for q_{aa} for deuteriums at positions 30 and 31, which is 5.6 kHz (3.3%) less than that for positions 32 and 33. Rotation of the chain about the O24–C25 bond to the second minimum at 85° leaves H(30) still close to H(16), and $q_{aa}(30)$ is barely changed in value at 164.3 kHz. The position of H(31), however, is now much further from H(16), and $q_{aa}(31)$ increases to a normal chain value of 168.4 kHz.

Note that in the liquid crystalline phases the observed quadrupolar splittings for sites 16 and 18 are equal because of rapid exchange of these positions produced by 180° flips of the rings about their para axes.

Values of q_{aa} and η were also calculated by B3LYP/6-311G** for conformers with a single gauche link corresponding to rotation about the bonds C24–C25, C25–C26, C26–C27 or C27–C28. In each conformer the changes produced in the values of the quadrupolar tensor components are $<1\%$.

To summarise, the calculations of the quadrupolar tensor components show that the assumption often made that the observed values of the quadrupolar splittings $\Delta\nu_k$ for positions along an alkyloxy chain attached to an aromatic core can be interpreted in terms of site, and conformationally independent values of $q_{aa}=168$ kHz and $\eta=0$ is valid to a precision of about 1%, except for the first and last carbons in the chain. For the first carbon, C24 in the case of 6OCB, the values of $q_{aa}=163$ kHz and $\eta=0.066$ should be used, whereas for the methyl deuteriums the values used should be $q_{aa}=173.0$ kHz and $\eta=0$. The assumption that $\eta=0$ except for the first position in the chain greatly simplifies the calculations of order parameters and conformational distributions whilst introducing an error probably less than 1%.

5. The structure, orientational order and conformational distribution of 6OCB

5.1. General

The measured dipolar couplings, D_{ij} , or quadrupolar splittings, $\Delta\nu_k$, are averages over all the conformations adopted by the molecules, and are given by equations (1)–(2), or their equivalents for a discrete set of

conformations. The quadrupolar tensor components in equation (6) will be assumed to be independent of the conformation, and so can be replaced by $q_{CD}(k)$ and $\eta(k)$ to give

$$\begin{aligned} \Delta\nu_k(n) = & \frac{3}{4}q_{CD}(k)[S_{zz}(n)\{(3\cos^2\theta_{azk}-1)+\eta(k)(\cos^2\theta_{bzk}-\cos^2\theta_{czk})\} \\ & + (S_{xx}(n)-S_{yy}(n))\{\cos^2\theta_{axk}-\cos^2\theta_{ayk} \\ & + \frac{1}{3}\eta(k)(\cos^2\theta_{bxk}-\cos^2\theta_{byk}-\cos^2\theta_{cxk}+\cos^2\theta_{cyk})\} \\ & + 4S_{xy}(n)\left\{\cos\theta_{axk}\cos\theta_{ayk}+\frac{1}{3}\eta(k)(\cos\theta_{bxk}\cos\theta_{byk}-\cos\theta_{cxk}\cos\theta_{cyk})\right\} \\ & + 4S_{xz}(n)\left\{\cos\theta_{axk}\cos\theta_{azk}+\frac{1}{3}\eta(k)(\cos\theta_{bxk}\cos\theta_{bzk}-\cos\theta_{cxk}\cos\theta_{czk})\right\} \\ & + 4S_{yz}(n)\left\{\cos\theta_{ayk}\cos\theta_{azk}+\frac{1}{3}\eta(k)(\cos\theta_{byk}\cos\theta_{bzk}-\cos\theta_{cyk}\cos\theta_{czk})\right\} \end{aligned} \quad (9)$$

The dipolar couplings in each conformation, $D_{ij}(n)$, are given by

$$\begin{aligned} D_{ij}(n) = & -K_{ij}(n)[S_{zz}(n)(3\cos^2\theta_{jz}-1)+(S_{xx}(n)-S_{yy}(n))(\cos^2\theta_{jix}-\cos^2\theta_{jyy}) \\ & + 4S_{xy}(n)\cos\theta_{jix}\cos\theta_{jyy}+4S_{xz}(n)\cos\theta_{jix}\cos\theta_{jz}+4S_{yz}(n)\cos\theta_{jyy}\cos\theta_{jz}] \end{aligned} \quad (10)$$

with

$$K_{ij}(n) = \mu_0\gamma_i\gamma_j h / 16\pi^3 r_{ijn}^3. \quad (11)$$

The vector r_{ijn} is aligned along the internuclear direction in conformation n , and makes angles θ_{ijx} , etc, with the reference axes xyz .

It is necessary to adopt a model for the conformational dependence of the order parameters, and to do this the additive potential (AP) model has been used [2]. This starts by defining a mean intermolecular potential, $U_{LC}(\beta, \gamma, n)$, for the molecule when in the n th conformation in the mean field of all other molecules, as

$$U_{LC}(\beta, \gamma, n) = U_{ext}(\beta, \gamma, n) + U_{int}(n). \quad (12)$$

The anisotropic part of this potential, $U_{ext}(\beta, \gamma, n)$, depends on the orientation of the molecules with respect to the mesophase director, which for uniaxial phases is defined by the polar angles β and γ . The form adopted for $U_{ext}(\beta, \gamma, n)$ is

$$U_{ext}(\beta, \gamma, n) = -\varepsilon_{2,0}(n)C_{2,0}(\beta) - 2\text{Re}\varepsilon_{2,2}(n)C_{2,2}(\beta, \gamma), \quad (13)$$

where the $C_{2,m}(\beta, \gamma)$ are modified spherical harmonics [23], and the $\varepsilon_{2,m}(n)$ are conformation-dependent interaction parameters. There are too many unknowns in equation (13) for it to be useful for molecules like 6OCB in which there are 121 distinct conformations for the alkyl chain alone. This problem is removed by expressing the $\varepsilon_{2,m}(n)$ as a tensorial sum of interaction coefficients, $\varepsilon_{2,p}(j)$, for each rigid subunit in the molecule:

$$\varepsilon_{2,m}(n) = \sum_q \sum_p \varepsilon_{2,p}(j) D_{p,m}^2(\Omega_{jn}), \quad (14)$$

where $D_{p,m}^2(\Omega_{jn})$ is the set of second-rank Wigner functions that describe the orientation of the j th subunit to the molecular reference frame in the n th conformation. Further simplifications are possible by equating interaction tensors for chemically-similar groups. The calculation proceeds by constructing an interaction tensor $\epsilon(n)$ in the molecular reference frame, diagonalizing this to produce components $\epsilon_{\alpha\beta}^P(n)$ in the principal frame, and then using these to calculate principal components of the conformation-dependent order parameters from:

$$S_{zz}^P(n) = Z(n)^{-1} \int \left(\frac{3}{2} \cos^2 \theta_{zq}(n) - \frac{1}{2} \right) \exp \left[\left\{ \epsilon_{2,0}^P(n) C_{2,0}(\beta) + 2 \operatorname{Re} \epsilon_{2,2}^P(n) C_{2,2}(\beta, \gamma) \right\} / RT \right] \sin \beta \, d\beta \, d\gamma \quad (15)$$

The partition function is

$$Z(n) = \int \exp \left[\left\{ \epsilon_{2,0}^P(n) C_{2,0}(\beta) + 2 \operatorname{Re} \epsilon_{2,2}^P(n) C_{2,2}(\beta, \gamma) \right\} / RT \right] \sin \beta \, d\beta \, d\gamma. \quad (16)$$

Having calculated the dipolar couplings or the quadrupolar splittings in the n th conformer, the averaged quantities are calculated from equations (1)–(2). To do this requires adopting a form for the probability, $P_{LC}(n)$, that the molecule is in the n th conformation, which is:

$$P_{LC}(n) = Q_{LC}^{-1} \int \exp[-U_{LC}(\beta, \gamma, n)/k_B T] \sin \beta \, d\beta \, d\gamma, \quad (17)$$

with

$$Q_{LC} = \sum_n \int \exp[-U_{LC}(\beta, \gamma, n)/k_B T] \sin \beta \, d\beta \, d\gamma. \quad (18)$$

Note that $P_{LC}(n)$ depends on both $U_{ext}(\beta, \gamma, n)$, the anisotropic mean potential, which vanishes in the isotropic phase, and $U_{int}(n)$, which does not. A probability, $P_{iso}(n)$ can be defined as:

$$P_{iso}(n) = Q_{iso}^{-1} \exp[-U_{int}(n)/k_B T] \quad (19)$$

with

$$Q_{iso} = \sum_n \exp[-U_{int}(n)/k_B T]. \quad (20)$$

It is important to note that $P_{iso}(n)$ may differ appreciably from $P_{LC}(n)$, the difference between the two increasing as the orientational order of the molecules increases.

The form adopted for $U_{int}(n)$ will depend on the conformational model being used, which in turn depends on how much data is available to test the model.

5.2. The structure, conformation and field-induced orientational order in the isotropic phase

5.2.1. The biphenyl group. There is very little information available to determine the structure or conformation of the biphenyl group in 6OCB when the sample is in the isotropic phase. This is because the four values of ${}^1D_{CH}^{induced}$ obtained for the biphenyl group and given in table 7 are exceeded by the number of unknown factors. Thus, the DFT and MP2 calculations both predict that rotation about the C5–O bond generates only the two, minimum-energy, planar forms, *A* and *B*, shown in figure 12.

The field-induced dipolar couplings between nuclei in the ring attached to the oxygen will be averaged over this motion so that

$$\begin{aligned} {}^1D_{ij}^{induced} = & -\frac{1}{2} K_{ij}(A) [S_{zz}(A) (3 \cos^2 \theta_{ijzA} - 1) \\ & + (S_{xx}(A) - S_{yy}(A)) (\cos^2 \theta_{ijxA} - \cos^2 \theta_{ijyA}) \\ & + 4S_{xz}(A) \cos \theta_{ijxA} \cos \theta_{ijzA}] \\ & -\frac{1}{2} K_{ij}(B) [S_{zz}(B) (3 \cos^2 \theta_{ijzB} - 1) \\ & + (S_{xx}(B) - S_{yy}(B)) (\cos^2 \theta_{ijxB} - \cos^2 \theta_{ijyB}) \\ & + 4S_{xz}(B) \cos \theta_{ijxB} \cos \theta_{ijzB}] \end{aligned} \quad (21)$$

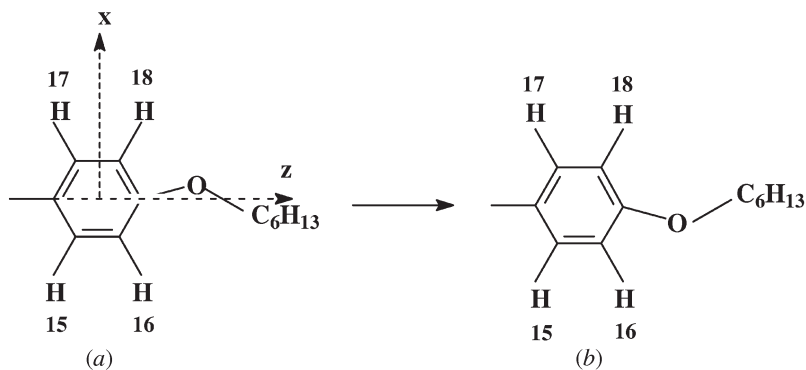


Figure 12. The two planar forms which are interchanged by rotation about the C5–O bond through 180°.

The axes xyz are fixed in the ring as shown in figure 12. The symmetry of this fragment means that:

$$\begin{aligned} S_{zz}(A) &= S_{zz}(B) = S_{zz}(R); \\ S_{xx}(A) &= S_{xx}(B) = S_{xx}(R); \\ S_{yy}(A) &= S_{yy}(B) = S_{yy}(R); \\ S_{xz}(A) &= -S_{xz}(B) = S_{xz}(R), \end{aligned}$$

with R signifying that these are local order parameters for use when the biphenyl fragment and not when the whole molecule is considered.

The number of unknown parameters therefore is 19 (three order parameters and 16 bond lengths and angles), compared with just four measured, field-induced couplings. Fixing all 16 geometrical parameters at those calculated by the B3LYP/6-311G** method, and given in table 8, reduces the number of unknowns to the three local order parameters, $S_{zz}(R)$, $S_{xx}(R)$ – $S_{yy}(R)$ and $S_{xz}(R)$. However, adjusting these three order parameters to bring the four calculated and observed couplings into best, least-squares agreement does not lead to acceptable agreement. The differences between calculated and observed values of the four values of ${}^1D_{CH}^{induced}$ are unacceptably large, which is because these couplings are very sensitive to the geometry and the order parameters. Increasing the variable parameters to include geometrical parameters is not possible as there is insufficient data to determine which changes in geometry are needed in order to bring the calculated couplings into agreement with those observed. This means that the ring geometry, or the local order parameters, cannot be obtained from the four ring couplings alone.

5.2.2. The conformation and orientational order of the alkyl chain in the isotropic phase. The total set of measured values of $D_{ij}^{induced}$ can be used to explore models for the chain conformations, and in addition give some information on the biphenyl group. The chains are assumed to exist in a set of conformations generated by rotations about the C–O, O–C and C–C bonds, taking into account only the minimum energy positions.

Rotation about the bond C5–O23 between the two forms coplanar with the attached ring will be accompanied by a compensating change in geometry, which makes this motion indistinguishable from a rotation through 180° about the z axis (see figure 12).

The minimum energy positions for the rest of the chain will at first be assumed to be those calculated by B3LYP/6-311G** and given in table 9.

The quantum chemical calculations that were done did not allow for long-range effects on the

conformational distribution, and to compensate in part for this neglect a steric term:

$$U^{steric}(n) = \sum_{i < j} A_{ij} / r_{ijn}^{12} \quad (22)$$

is added to $U_{int}(n)$, where the summation is over hydrogen atoms separated by more than three bonds only, and A_{ij} is given a value of $1.1 \text{ J } \text{\AA}^{12}$ [24], which is sufficient to eliminate severely hindered conformations.

The rings, when coplanar are assumed to have yz as a mirror plane, and the angle that C9–H20 (and C11–H21) makes with the z axis is fixed at the value calculated by B3LYP/6-311G** (120.06°). The angles that the other three pairs of symmetry related C–H bonds make with z are then treated as variables.

In the AP model it is necessary to choose interaction tensors for the rigid units in the biphenyl group and in the alkyloxy chain. For the biphenyl group, the structure of which is symmetrized by making the x coordinates of 15, 16, 21 and 22 equal, and equal but opposite in sign to those of 17, 18, 19 and 20, it is sufficient to use ϵ_{zz} and $\epsilon_{xx} - \epsilon_{yy}$. In the calculations by the AP method by Counsell *et al.* [3] on the quadrupolar splittings for deuteriums in 6OCB- d_{15} in the nematic phase it was decided to use just a single interaction tensor component, ϵ_{CC} , for each O–C or C–C bond, identical for all bonds. This parameterization is also tried here, using just the ten values of ${}^1D_{CH}^{induced}$ as the data to be fitted by varying the three interaction parameters and the three ring angles. The values of ${}^1D_{CHk}$ dipolar couplings, both in isotropic and liquid crystalline phases, and deuterium quadrupolar splittings, $\Delta\nu_k$, for the same site in the aliphatic chain and for the same temperature are expected to be approximately linearly related [8]. The calculated values of ${}^1D_{CH}^{induced}$ for the chain positions follow the trend of those observed, and in particular ${}^1D_{26,34}^{induced} = {}^1D_{26,35}^{induced} < {}^1D_{27,36}^{induced} = {}^1D_{27,37}^{induced}$. This suggests that the relative magnitudes of either the dipolar couplings or the quadrupolar splittings at positions C26 and C27 is primarily determined by the preference for the gauche conformations for rotation about C24–C25. However, the calculated values of ${}^2D_{30,31}^{induced}$ and ${}^2D_{32,33}^{induced}$ are almost double the observed values, and so the model is not yet correct. This problem was solved by re-examining the choice of the interaction parameters for the chain segments. The rigid segments are the units shown in figure 13.

Each fragment is assumed to have C_{2v} symmetry and therefore to have principal components for the local interaction tensor of $\epsilon_{C\dots C}$, which is directed along $C_k\dots C_{k+2}$ or $O\dots C_{25}$, and ϵ_{HH} , which acts along the $H\dots H$ directions.

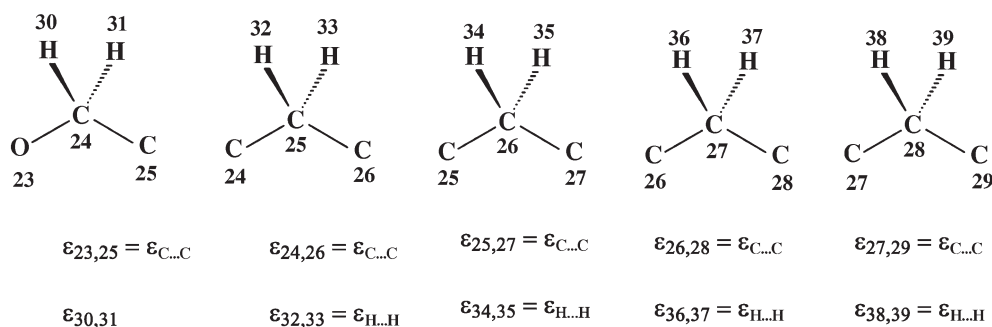


Figure 13. Rigid segments and the interaction parameters for the alkyloxy chain of 6OCB.

A good fit to the data was found by varying five interaction parameters, three angles in the biphenyl group, and the angle $C5O23C24$ compared with 11 dipolar couplings to give the results in table 11.

Improvements to the fit can undoubtedly be made by changes in the geometry or the values of E_{fg} , but there are insufficient data to obtain a unique solution in this way. It should also be noted that vibrational averaging of the values of $D_{ij}^{induced}$ has been neglected, and this could affect significantly the calculated couplings, and hence the fitting parameters.

6. The structure, conformation and orientational ordering of 6OCB in the liquid crystalline phases

6.1. The biphenyl group

The data obtained from the 1H - $\{^2H\}$ and 2H spectra of pure 6OCB and in the mixture with EBBA is of a much greater precision to that obtained for the isotropic phase, and particularly for the biphenyl group, is able to give much more precise information on structure and conformation. Thus, the dipolar couplings between the protons in the biphenyl group can be used to determine the relative positions of the protons, the local order parameters for the group, and $P_{LC}(\phi_R)$, the probability distribution of ϕ_R , the inter-ring angle. It is assumed that the bond lengths and angles in the molecule do not change with temperature or phase, and all four sets of data are used to obtain a common geometry for the proton framework in the biphenyl group. The values of the dipolar couplings between protons in each of the phenyl groups are averaged by 180° ring flips, which means that it is not possible to distinguish between interconversion of forms with the asymmetric structures predicted by the B3LYP calculations, with a geometrical relaxation on rotation, and a symmetric ring structure with symmetry C_{2v} , and so this effective, symmetric structure was adopted. To obtain a common geometry it is necessary to fix at least one distance. The distance $r_{15,17}=4.295 \text{ \AA}$ was fixed, which is the value

calculated by B3LYP/6-311G**. The distances $r_{19,20}=r_{21,22}$ and the angles $\theta_{20,9,8}=\theta_{21,11,12}$, which are now, in the symmetric structure, those between the C–H

Table 11. The interaction parameters, ϵ_{ij}/RT , the angles θ_{ijz} between atoms i, j and z and the angle $\theta_{5,23,24}$ obtained by fitting calculated to observed values of the field-induced dipolar couplings, $D_{ij}^{induced}$, for 6OCB in the isotropic phase at 348.1 K. The local order parameters, $S_{zz}(R)$ and $S_{xx}(R)-S_{yy}(R)$, are also given.

| i, j | $D_{ij}^{induced} / \text{Hz}$ | |
|--|--------------------------------|------------|
| | observed | calculated |
| 3, 15 | 2.90 | 2.90 |
| 4, 16 | 2.25 | 2.25 |
| 8, 19 | 4.15 | 4.15 |
| 9, 20 | 2.90 | 2.90 |
| 24, 30 | 10.32 | 10.31 |
| 25, 32 | 9.27 | 9.48 |
| 26, 34 | 7.60 | 7.15 |
| 27, 36 | 7.75 | 7.60 |
| 28, 38 | 4.58 | 5.12 |
| 29, 40 | 2.50 | 2.39 |
| 30, 31 | 6.60 | 6.62 |
| 32, 33 | 6.20 | 6.21 |
| Interaction parameters, ϵ_{ij}/RT | | |
| 1, 2 | 0.0090 ± 0.0006 | |
| 3, 7 | 0.0038 ± 0.0004 | |
| 23, 25=24, 26=25, 27=26, 29=27, 29 | 0.00216 ± 0.00009 | |
| 30, 31 | 0.0046 ± 0.0004 | |
| 32, 33=34, 35=36, 37=38, 39 | 0.0014 ± 0.0001 | |
| Angles $\theta_{ijz}/^\circ$ | | |
| 3, 15 | 119.9 ± 0.4 | |
| 4, 16 | 120.9 ± 0.4 | |
| 8, 19 | 121.6 ± 0.4 | |
| 5, 23, 24 | 126.8 ± 1.4 | |
| $S_{zz}(R)$ | 0.00152 | |
| $S_{xx}(R)-S_{yy}(R)$ | 0.00018 | |

Table 12. The distances $r_{19,20}=r_{21,22}$, the angles $\theta_{15,3,4}=\theta_{17,7,6}$ and the local order parameters $S_{zz}(R)$ and $S_{xx}(R)-S_{yy}(R)$ that are in best agreement with the dipolar couplings for the sample of 6OCB- d_{15} in the nematic phase, and in the mixture with EBBA in the SmA and SmB phases.

| Distances and angles | | Order parameters | | | |
|--|-------------------|------------------------|-------------------|----------------------|-------------------|
| | | 6OCB- d_{15} nematic | | 6OCB- d_{15} /EBBA | |
| | | 323 K | SmA 347 K | SmB 337 K | 327 K |
| $r_{19,20}=r_{21,22}/\text{\AA}$ | 2.490 ± 0.011 | | | | |
| $\theta_{20,9,8}=\theta_{21,11,12}/^\circ$ | 119.1 ± 0.6 | | | | |
| $S_{zz}(R)$ | 0.676 ± 0.001 | | 0.874 ± 0.001 | 0.950 ± 0.001 | 0.955 ± 0.001 |
| $S_{xx}(R)-S_{yy}(R)$ | 0.062 ± 0.005 | | 0.049 ± 0.005 | 0.040 ± 0.005 | 0.041 ± 0.005 |

bonds and the z axis, were varied to bring the calculated values of the couplings $D_{15,17}$, $D_{19,20}=D_{21,22}$, $D_{19,22}$, $D_{20,21}$, $D_{19,21}=D_{20,22}$ into best least squares agreement with the two geometrical parameters and local order parameters $S_{zz}(R)$ and $S_{xx}(R)-S_{yy}(R)$. This gave the results shown in table 12.

The geometry was then fixed and the inter-ring couplings used to explore the form of $P_{LC}(\phi_R)$ and $P_{iso}(\phi_R)$, the probability distributions for the conformations generated by rotation about the inter-ring C-C bond. Most previous studies of these probability distributions for biphenyl fragments [21, 22, 25] have used a cosine expansion for the bond rotational potential, and hence for $U_{int}(\phi_R)$, such as:

$$U_{int}(\phi_R) = V_2 \cos 2\phi_R + V_4 \cos 4\phi_R. \quad (23)$$

However, although equation (23) gives the correct periodicity of the rotation potential it restricts the curve to having a shape which may be incorrect. Thus, the position of the minimum energy, ϕ_{min} , depends only on the ratio V_2/V_4 :

$$\phi_{min} = \frac{1}{2} [\cos^{-1}(-V_2/4V_4)]. \quad (24)$$

When $V_2=0$ the potential has a minimum at 45° , and $U_{iso}(0^\circ)=U_{iso}(90^\circ)$. For $\phi_{min}<45^\circ$, the value of V_2 is negative, and $V(0^\circ)<V(90^\circ)$, and for $\phi_{min}>45^\circ$, the value of V_2 is positive, and $V(0^\circ)>V(90^\circ)$. Including more terms in equation (23) will remove this correlation between the values of ϕ_{min} , $V(0^\circ)$ and $V(90^\circ)$, as also does adding repulsions between the hydrogen atoms at positions 15, 17, 19 and 22, but a simpler way of having a more flexible form for $U_{iso}(\phi_R)$ is to express the probability $P_{iso}(\phi_R)$ as a sum of Gaussian functions [26]:

$$P_{iso}(\phi_R) = [8\pi h^2]^{-\frac{1}{2}} \left[\exp\left(-\{\phi_R - \phi_{min}\}^2 / 2h^2\right) + \exp\left(-\{\phi_R - 180 - \phi_{min}\}^2 / 2h^2\right) \right] \quad (25)$$

with h being the width at half maximum height. This approach is similar to that based on the maximum entropy principle and introduced by Zannoni [27].

Both the ‘‘Fourier’’, equation (23), and the ‘‘direct probability’’, equation (25), approaches to representing $P_{iso}(\phi_R)$ do not allow for the effect of short-range repulsion on the bond rotation probability distribution. This may be introduced into both methods by a term

$$P_{rep}(\phi_R) = \exp[-U_{steric}(\phi_R)/RT], \quad (26)$$

where U_{steric} is given by equation (22).

The AP model was used to construct $U_{ext}(\beta, \gamma, \phi_R)$ using interaction parameters ϵ_{zz}^R and $\epsilon_{3,7}^R = \epsilon_{8,12}^R$, the superscript R signifying that these are for use for the biphenyl fragment and not when the whole molecule is considered. The probability densities $P_{iso}(\phi_R)$ and $P_{LC}(\phi_R)$ differ since the latter has a contribution from the anisotropic potential. This means that ϕ_{min}^{LC} , the maximum in $P_{LC}(\phi_{ring})$, will differ from ϕ_{min} , the maximum in $P_{iso}(\phi_R)$. One of the advantages of the AP model is that both these angles are determined by fitting the calculated to observed dipolar couplings, and are given in table 13 together with the other fitting parameters. The distributions are shown in figure 14, which clearly reveals the strong effect of the anisotropic potential on $P_{LC}(\phi_R)$ in the smectic phases.

Note the large values obtained for ϵ_{zz}^R and $\epsilon_{3,7}^R = \epsilon_{8,12}^R$ in the SmB phase, which is because ϵ_{zz}^R will tend to infinity as S_{zz} approaches unity. This phenomenon also produces large error limits on these parameters in the fitting process, but not large errors on $S_{zz}(R)$ and $S_{xx}(R)-S_{yy}(R)$, the values of which are given in table 12.

The value of ϕ_{min} is found to be almost unchanged by increasing the orientational order at a mean value of 34° , compared with the calculated values of 37.12° by B3LYP/6-311G* and 43.17° by MP2/6-31G*; the latter calculated value probably corresponds the most closely to that in an isolated molecule of 6OCB, a conclusion

Table 13. The interaction parameters ϵ_{zz}^R and $\epsilon_{3,7}^R = \epsilon_{8,12}^R$, in units of RT , and the values of h , ϕ_{min}^{LC} and ϕ_{min} , the parameters defining the probability distribution for rotation about the inter-ring bond for the biphenyl fragment obtained by fitting calculated to observed values of dipolar couplings of 6OCB- d_{15} in the nematic phase at 323 K, and in the mixture with EBBA in SmA (347 K) and SmB phases (337 and 327 K).

| | 6OCB- d_{15} /EBBA | | | |
|--|------------------------|----------------|--------------|--------------|
| | 6OCB- d_{15} nematic | SmA | SmB | SmB |
| | 323 K | 347 K | 337 K | 327 K |
| ϵ_{zz}^R | 4.78 ± 0.07 | 15.6 ± 1.3 | 83 ± 37 | 102 ± 48 |
| $\epsilon_{3,7}^R = \epsilon_{8,12}^R$ | 0.99 ± 0.06 | 5.3 ± 0.8 | 38 ± 19 | 48 ± 25 |
| $\phi_{min} / ^\circ$ | 34.8 ± 0.2 | 34.0 ± 0.3 | 34 ± 2 | 35 ± 3 |
| $\phi_{min}^{LC} / ^\circ$ | 36 ± 0.5 | 33 ± 0.5 | 30 ± 0.5 | 28 ± 0.5 |
| $h / ^\circ$ | 16 ± 1 | 21 ± 2 | 21 ± 2 | 24 ± 3 |

based on the good agreement obtained for the value of ϕ_{min} calculated by MP2/6-31G* for biphenyl of 46° [28] and that measured by electron diffraction of a gaseous sample of 44.4° [12]. A study of ϕ_{min} for biphenyl in a liquid crystalline solvent obtained values of 37° when

using the AP model, and 34° when the same data was treated by the maximum entropy method [21].

The increase in the difference between ϕ_{min}^{LC} and ϕ_{min} for 6OCB from essentially zero in the nematic phase to 7° in the SmB at 327 K is very similar to the difference

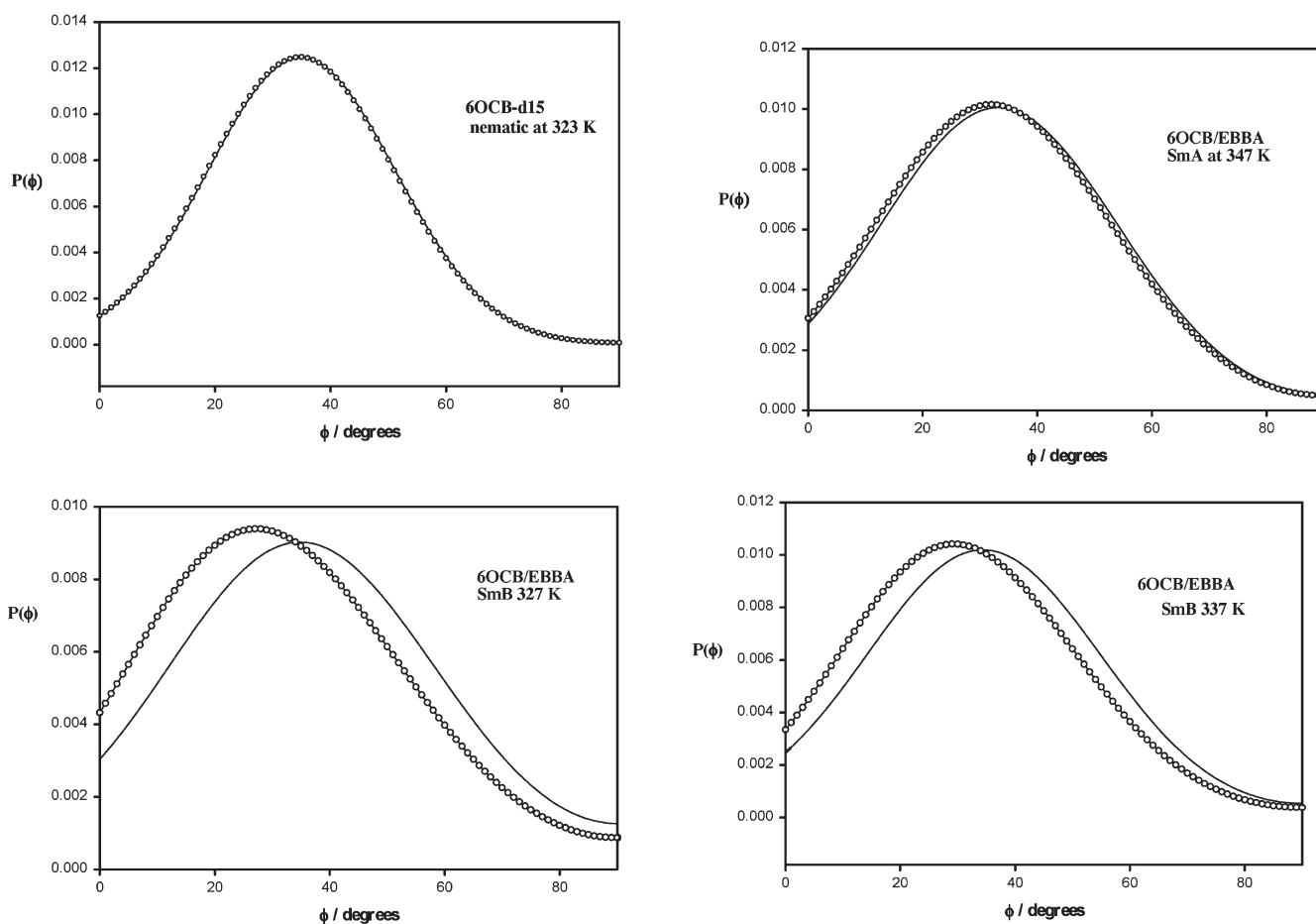


Figure 14. The probability distributions $P_{LC}(\phi_R)$, circles, and $P_{iso}(\phi_R)$, continuous line, for rotation about the inter-ring bond in the biphenyl group of 6OCB.

found for the fixed values of the inter-ring angle of 36° and 26° for the two different molecules in the unit cell of the crystalline form of 6OCB [18].

6.2. The conformational distribution for the alkyloxy chain in 6OCB and 6OCB/EBBA in the liquid crystalline phases determined from the deuterium quadrupolar splittings

The procedure for testing models for $P_{LC}(n)$ for the conformations adopted by the alkyloxy chain is similar to that used for the isotropic phase in that the RIS model is adopted together with the AP method of predicting the conformational dependence of the orientational order. However, the data set for the liquid crystalline phases is different being a combination of dipolar couplings between protons in the biphenyl fragment, and quadrupolar splittings for deuterium nuclei in the chain positions. The values of D_{ij} between protons in the same phenyl group are used and not the

inter-ring couplings since the latter do not affect the derivation of either $P_{LC}(n)$ for the chain, or the orientational order parameters. The values used for $q_{CD}(k)$ in equation (9) in order to calculate the splittings $\Delta\nu_k(n)$ are those in column B of table 10, and $\eta(k)$ is set to zero for all sites in the chain.

It was found possible to bring calculated and observed data into good, but not exact, agreement by assuming the geometry of the ring is that in table 12, and of the rest of the molecule to be that calculated by the B3LYP/6-311G** method and given in table 8, and the values of $E_{lg}(k)$ to be those in table 9. The interaction parameters used were the set given in figure 13 and adopted to fit data for the isotropic phase. Figure 15 shows the values of the C–D bond order parameters, $S_{CD}(k)$ calculated with this model compared with the observed values.

The observed and calculated values are in quite good agreement for the pure sample in the nematic phase, but

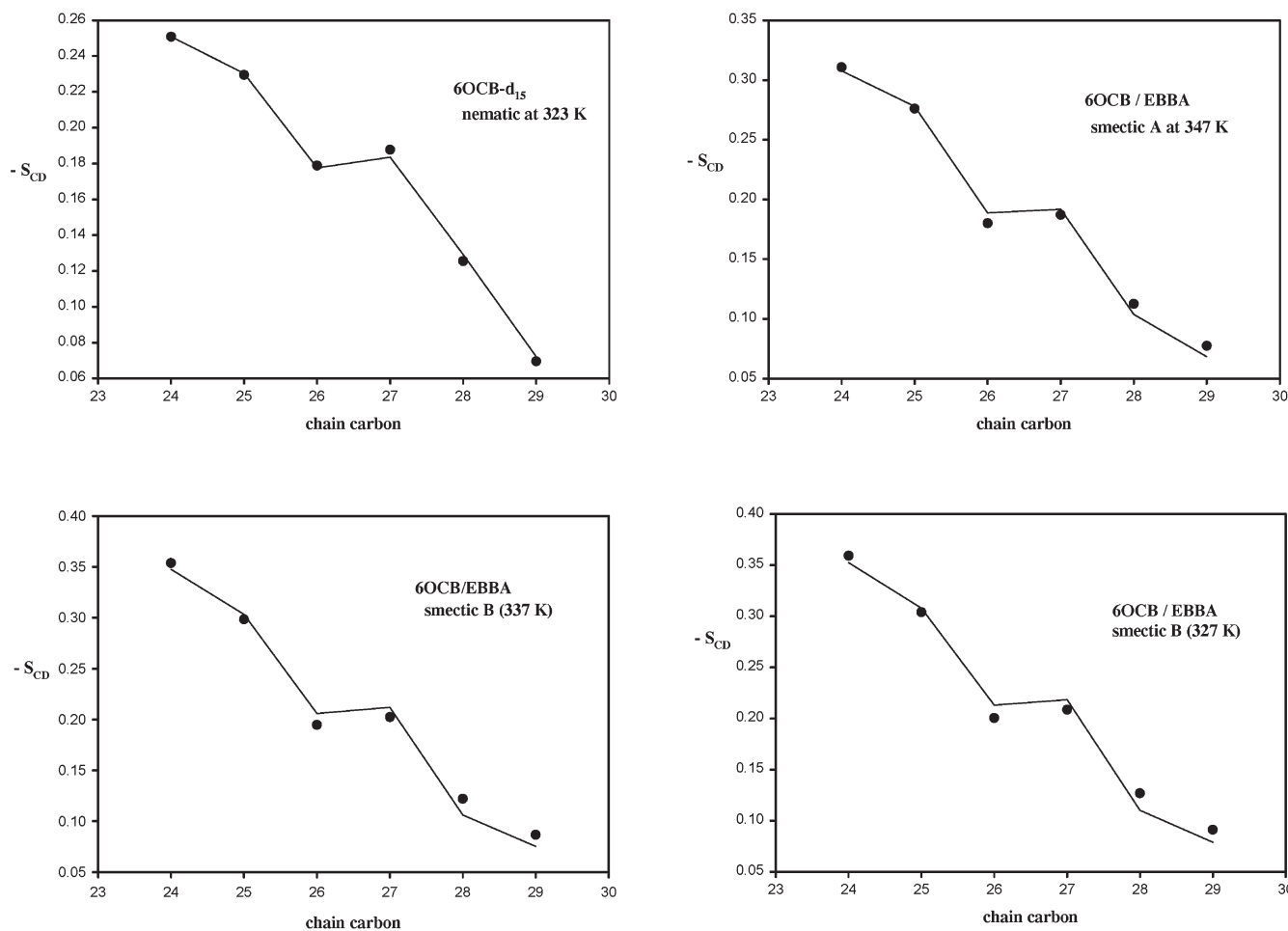


Figure 15. Variation of the C–D bond order parameter, $S_{CD}(k)$, with chain position. The observed values (joined by the continuous line) are compared with those calculated (●) using the AP model with the geometry and the bond rotational parameters E_{lg} fixed at those obtained by B3LYP/6-311G**.

the agreement is much worse for the mixture with EBBA particularly for the last three positions in the chain. This suggests that the conformational distribution is significantly different in the mixed samples, although this could also be because the samples are in smectic phases.

The calculated data sets were brought into very good agreement with those observed by varying the values of $E_{ig}(O-C24)$, $E_{ig}(C24-C25)$ and $E_{ig}(C25-C26)=E_{ig}(C26-C27)=E_{ig}(C27-C28)$, with the results shown in table 14.

6.3. The effects of the phase on the conformational distributions

The RIS approximation for the probability distribution greatly simplifies the fitting of calculated to observed quadrupolar splittings or dipolar couplings, but there are still too many conformers, 243 in the alkyloxy chain, to be easily visualized. Figure 16 shows just the populations of the 11 most populated conformers, where the twofold degeneracy of conformers containing at least one gauche form has been taken into account.

In the isotropic phase the conformer $tgttt$ (and its degenerate form $tg-ttt$) are the most populated single forms, whereas the singly-degenerate form $ttttt$ is similar in population to those with a single gauche form. Also in the isotropic phase the distributions $P_{iso}(n)$ and $P_{LC}(n)$ are essentially identical. On entering the nematic phase these two distributions become substantially different, there being a more than doubling of $P_{LC}(ttttt)$ compared with $P_{iso}(ttttt)$ and this isomer becomes almost as populated as $tgttt$. This trend is continued into the SmA and SmB phases, where now the $ttttt$ form is the most populated conformer. Note that $P_{LC}(ttttt)$ in the different phases does not change

appreciably, but some of the other conformers, particularly $gtttt$, dramatically decrease.

7. Conclusion

The experiments reported here show that it is possible to obtain the conformation, structure and orientational order for a molecule such as 6OCB over almost the complete range of orientational order of the molecules. Earlier work on 6OCB [3] assumed that the most favoured conformation in the nematic phase is the all-trans form whereas it is now shown that in both isotropic and nematic phases the most populated degenerate pair are $tgttt$ and $tg-ttt$. The molecules in the solid, crystalline phase are in the $ttttt$ form which gradually becomes the dominant single form in the smectic phases formed by mixing 6OCB with EBBA.

It should of course be remembered that these conclusions depend on a number of assumptions which have been made in order to analyse the NMR data. The NMR data can determine the probability distribution $P_{LC}(\phi_R)$ for rotation about the inter-ring bond in the liquid crystalline phases with the most confidence, because of the sensitivity of the values of D_{ij} between the protons in the biphenyl fragment to the form of this function. The model used to analyse the data, the AP model, leads to the prediction that $P_{LC}(\phi_R)$ changes appreciably as the orientational order increases, and that there is a progressive reduction in the minimum energy position, ϕ_{min}^{LC} .

The conformational distributions obtained for the alkyloxy chain in all phases are more dependent on the bond angles assumed for the chain, and also on the adoption of the RIS model for the conformational distributions. The geometry was taken from the DFT calculations, which it is suggested is the best practical

Table 14. The interaction parameters, ϵ_{zz} , $\epsilon_{3,7}$, ϵ_{CC} , ϵ_{HH} and $\epsilon_{30,31}$, in units of RT , and the energy differences $E_{ig}(i,j)$ between *trans* and *gauche* forms generated by rotation about the ij th bond obtained by fitting calculated to observed dipolar couplings and quadrupolar of 6OCB- d_{15} in the nematic phase at 323 K, and in the mixture with EBBA in SmA (347 K) and SmB phases (337 and 327 K).

| | 6OCB- d_{15} /EBBA | | | |
|---|------------------------|-------------------|------------------|------------------|
| | 6OCB- d_{15} nematic | SmA | SmB | SmB |
| | 323 K | 347 K | 337 K | 327 K |
| ϵ_{zz} | 6.1 ± 0.6 | 15.4 ± 0.7 | 38 ± 7 | 39 ± 6 |
| $\epsilon_{3,7}$ | 4.0 ± 0.7 | 10.3 ± 0.8 | 28 ± 7 | 27 ± 6 |
| $\epsilon_{C...C}$ | 0.89 ± 0.02 | 0.775 ± 0.007 | 0.89 ± 0.02 | 0.87 ± 0.02 |
| ϵ_{HH} | 0.69 ± 0.02 | 0.454 ± 0.008 | 0.45 ± 0.02 | 0.40 ± 0.02 |
| $\epsilon_{30,31}$ | 2.4 ± 0.5 | 3.3 ± 0.2 | 1.1 ± 0.3 | 0.4 ± 0.3 |
| $E_{ig}(O-C24)$ | -10.2 ± 1.4 | -14.1 ± 0.5 | -6.69 ± 0.08 | -4.5 ± 0.8 |
| $E_{ig}(C24-C25)$ | 0.95 ± 0.08 | -0.41 ± 0.02 | 0.40 ± 0.02 | -0.47 ± 0.02 |
| $E_{ig}(C26-C27)=E_{ig}(C27-C28)=E_{ig}(C28-C29)$ | -4.04 ± 0.02 | -2.64 ± 0.01 | -1.88 ± 0.02 | 1.81 ± 0.02 |

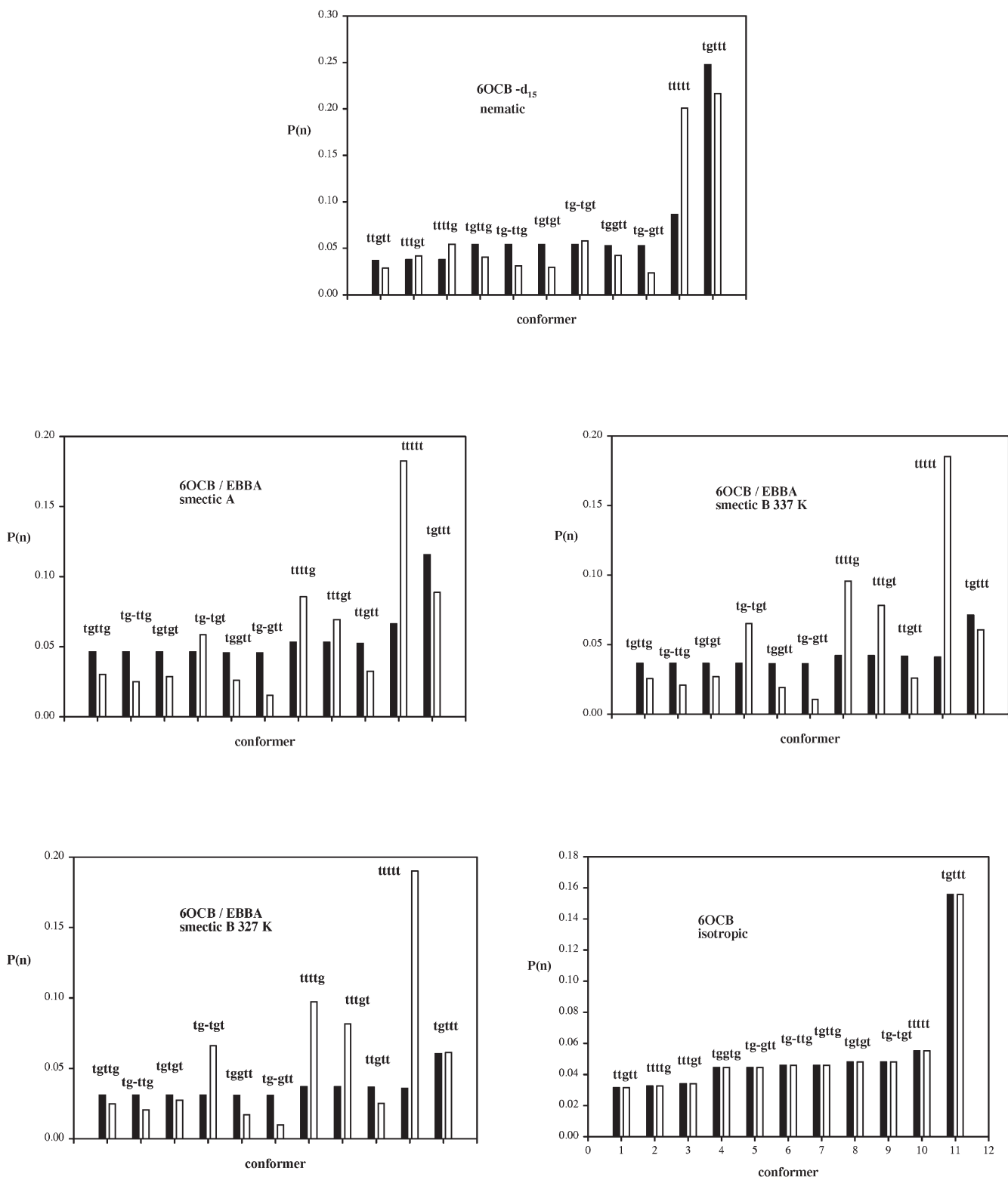


Figure 16. Most populated conformers of 6OCB. The labelling $tg-tgt$, etc, signifies whether a $X_{k-2}-X_{k-1}-X_k-X_{k+1}$, were X is O or C and k starts at C24, is *trans* (t), *gauche+* (g), or *gauche-* (g-). The filled bars are for $P_{iso}(n)$, and unfilled for $P_{LC}(n)$.

procedure for obtaining this information for large molecules for use in interpreting liquid state data. The assumption that a distribution between only minimum energy forms can represent the conformational flexibility of the chain is probably the most serious approximation used in analyzing the data. To improve on this approximation in iterative fitting of data is as yet beyond the capacity of current day computing resources, and hence the RIS model is forced upon us as the best that can be tested.

References

- [1] J.W. Emsley, G.R. Luckhurst. *Mol. Phys*, **41**, 19 (1980).
- [2] J.W. Emsley, G.R. Luckhurst, C.P. Stockley. *Proc. R. Soc. A*, **381**, 117 (1982).
- [3] C.J.R. Counsell, J.W. Emsley, G.R. Luckhurst, H.S. Sachdev. *Mol. Phys*, **63**, 33 (1988).
- [4] C.D. Poon, C.M. Woolbridge, B.M. Fung. *Mol. Cryst. liq. Cryst*, **157**, 303 (1988).
- [5] J.W. Emsley, E.K. Foord, P.J.F. Gandy, D.L. Turner, H. Zimmermann. *Liq. Cryst*, **17**, 303 (1994).
- [6] G. Celebre, G. De Luca, M. Longeri, E. Sicilia. *J. Chem. Inf. Comput. Sci*, **34**, 539 (1994).
- [7] W. Bruigel. *NMR Spectra and Chemical Structure*. Academic Press, New York (1967).
- [8] D. Merlet, A. Lesage, J.W. Emsley. *J. phys. Chem. A*, **109**, 5070 (2005).
- [9] J. Farjon, D. Merlet, P. Lesot, J. Courtieu. *J. magn. Resonance*, **158**, 169 (2002).
- [10] *GAUSSIAN 03 (Revision C.02)*. Gaussian Inc, Wallingford CT (2004).
- [11] A. Goller, U.-W. Grummt. *Chem. Phys. Lett*, **321**, 399 (2000).
- [12] A. Almendingen, O. Bastiansen, L. Fernholt, B.N. Cyvin, S. Cyvin, S. Samdal. *J. Mol. Struct*, **128**, 115 (1985).
- [13] J.M. Granadino-Roldán, M. Fernández-Gómez, A. Navarro. *Chem. Phys. Lett*, **372**, 255 (2003).
- [14] J.C. Cochrane, K. Hagen, G. Paulen, Q. Shen, S. Tom, M. Traetteberg, C. Wells. *J. Mol. Struct*, **413**, 313 (1997).
- [15] G. Celebre, G. De Luca, M. Longeri, G. Pileio, J.W. Emsley. *J. chem. Phys*, **120**, 7075 (2004).
- [16] G. Celebre, De Luca G, Longeri M., Emsley J.W., *J. phys. Chem*, **96**, 2466 (1992).
- [17] D.C. Spellmeyer, P.D.J. Grootenhuis, M.D. Miller, L.F. Kuyper, P.A. Kollman. *J. phys. Chem*, **94**, 4483 (1990).
- [18] K. Hori, Y. Koma. *Mol. Cryst. liq. Cryst*, **225**, 15 (1993).
- [19] L.J. Burnett, B.H. Muller. *J. chem. Phys*, **55**, 5829 (1971).
- [20] W.C. Bailey. *J. Mol. Spectrosc*, **190**, 318 (1998).
- [21] G. Celebre, G. De Luca, M. Longeri, D. Catalano, C.A. Veracini, J.W. Emsley. *J. chem. Soc., Faraday Trans*, **87**, 2623 (1991).
- [22] J.W. Emsley, T.J. Horne, G. Celebre, G. De Luca, M. Longeri. *J. chem. Soc., Faraday Trans*, **88**, 1679 (1992).
- [23] D.M. Brink, G.R. Satchler. *Angular Momentum*, second edn, Oxford University Press, Oxford (1968).
- [24] J.W. Emsley. *Phys. Chem. chem. Phys*, **8**, 3726 (2006).
- [25] J.W. Emsley, G. Celebre, G. De Luca, M. Longeri, F. Luchesini. *Liq. Cryst*, **16**, 1037 (1994).
- [26] G. Celebre, G. De Luca, J.W. Emsley, E.K. Foord, M. Longeri, F. Luchesini, G. Pileio. *J. chem. Phys*, **118**, 6417 (2003).
- [27] C. Zannoni. In *NMR of Liquid Crystals* Chap. 2, Reidel, Dordrecht (1985).
- [28] F. Grein. *J. Mol. Struct. (Theochem)*, **624**, 23 (2003).